Wetlands (2024) 44:101
https://doi.org/10.1007/s13157-024-01855-y

WETLAND ECOSYSTEMS, PAST, PRESENT AND FUTURE

Dynamic Change Characteristics of Wetlands in Hefei and their Driving Factors Along the Urban–Rural Gradient

Hui Zhang[1] · Chuntao Li[1] · Yichen Zhang[2] · Lang Zhang[3]

Received: 22 April 2024 / Accepted: 26 August 2024

Abstract

Wetlands, as vital components of urban ecological infrastructure, provide essential ecosystem services. However, they face increasing risks of degradation and loss due to their vulnerability, environmental changes, and human activities. Therefore, effective restoration efforts are urgently needed. This study adopts a novel approach by considering the urban–rural gradient and integrates land use data, ecological parameters, and anthropogenic factors in Hefei City. Through morphological spatial pattern analysis, principal component analysis, and affinity propagation, this study identifies and analyzes urban–rural gradients. Using the optimal parameter geographic detector, the drivers of wetland changes from 1990 to 2020 are quantitatively assessed across different urban–rural gradients in Hefei. The findings indicate the following. (1) A persistent reduction in wetland expanse throughout the study duration, diminishing from 1274.56 km^2 in 1990 to 1119.37 km^2 in 2020, constituting a decrement of 12.17%. (2) Based on geographic detector outcomes, disparate driving forces underpin wetland dynamics across urban–rural gradients, with urban locales predominantly influenced by organic carbon and the proportion of impervious surface factors. Meanwhile, in agricultural and semi-ecological villages, silt is the primary factor, while ecological villages are primarily modulated by both silt and gross domestic product factors. Additionally, synergistic interactions manifest heightened explanatory power. This study elucidates the mechanistic underpinnings of wetland dynamics along urban–rural gradients, providing pivotal insights for developing targeted wetland restoration and conservation policies pertinent to the urban–rural developmental trajectory in Hefei City. Concurrently, it offers relevant recommendations for the multifaceted stewardship and sustainable development of wetlands in Hefei City in the foreseeable future.

Keywords Urban–rural gradient · Urban wetland · Dynamic change characteristic · Drivers of change · Optimal parameter geographic detector

✉ Chuntao Li
lichuntao@ahau.edu.cn

Hui Zhang
zhang_hui@stu.ahau.edu.cn

Yichen Zhang
zhangyichen@hainanu.edu.cn

Lang Zhang
zl@shsyky.com

[1] School of Forestry and Landscape Architecture, Anhui Agricultural University, Hefei 230036, China

[2] School of Ecology and Environment, Hainan University, Haikou 570228, China

[3] Shanghai Academy of Landscape Architecture Science and Planning, Shanghai 200232, China

Introduction

Wetlands, which are recognized as distinctive ecosystems, link terrestrial ecosystems with aquatic ecosystems (Cong et al. 2019; Salimi et al. 2021). They are also recognized as the “natural gene bank” (Bian et al. 2020; Zhou et al. 2009), and hold immense importance for hydrological regulation, climate moderation, biodiversity conservation, and water purification (Kumari et al. 2020; Liu et al. 2018a; Meng et al. 2017). At the same time, wetlands are recognized as one of the most delicate ecosystems on Earth. It is estimated that over half of wetlands globally have experienced degradation or disappearance as a result of the synergy between anthropogenic disturbances and variability in their ecological surroundings (Davidson 2014; Desta et al. 2012; Kirwan and Megonigal 2013). Wetland areas have been repeatedly occupied and destroyed by China's rapid urbanization and

Published online: 18 September 2024

industrialization after its reform and opening up (Zhao et al. 2019; Mao et al. 2018). Concurrently, industrial pollution, domestic wastewater, and aquaculture have hastened the degradation of wetlands (Bian et al. 2020). The growing conflict between urban construction and wetland ecological conservation has been increasingly pronounced in this process. Urban wetlands serve multifaceted functions, such as alleviating the heat island effect and preventing floods and droughts (McLaughlin and Cohen 2013; Xue et al. 2019). They are essential in creating environmentally friendly cities and promoting sustainable development (Peng et al. 2020). Therefore, a comprehensive exploration of urban wetlands' spatial and temporal evolution characteristics, coupled with an in-depth investigation into their driving mechanisms, is crucial to promoting urban wetland management and sustainable development.

The dynamic changes in urban wetlands stem from the synergistic impact of various indicators, categorized into two primary dimensions: ecological surroundings and anthropogenic interventions (van Asselen et al. 2013; Xiong et al. 2023). Ecological surrounding factors include climate, soil properties, and terrain. Climate can impact wetland ecosystems through temperature elevation and alterations in hydrological patterns (Erwin 2009). Precipitation is the primary source of recharge for wetlands, and it has a direct impact on their formation and growth by influencing the distribution of water resources in terms of both time and space (Erwin 2009). At the same time, evapotranspiration and temperature influence the distribution of wetlands by influencing water circulation (Havril et al. 2018). Soil properties affect the ecosystem structure and function of wetlands. Studies have found that the soil's water-holding capacity increases with higher levels of organic carbon content (Masood and Ali 2023; Wang et al. 2020). In contrast, sand has a weaker water-holding capacity than clay, making it easier for water to penetrate and difficult to form a wetland (Herawati et al. 2021; Riaz and Marschner 2020). The soil's pH level influences vegetation and is a pivotal factor influencing the formation and spatial distribution of wetlands (Liu et al. 2018b). It governs the distribution of relatively depressed landforms within the region, thereby influencing the character of regional water flow (Jin et al. 2017; Job and Sieben 2022). Anthropogenic interventions, such as changes in land use, directly affect wetlands and also indirectly affect them by influencing ecological surrounding factors (Maneas et al. 2019; Newton et al. 2020).

Different levels of urbanization across distinct urban–rural gradients correspond to different levels of human pressure on wetland ecosystems. However, most existing studies on the dynamic change mechanisms of urban wetlands analyze the correlation between wetland dynamics and its drivers from the perspective of the entire region (Long et al. 2022; Wang et al. 2022; Zhang et al. 2021b). This approach may overlook crucial details. Thus, analyzing the response of urban wetland dynamic change to various drivers from the perspective of subdivided geographical space is of great significance. Urban–rural gradient analysis is widely employed in ecological studies (Hou et al. 2020; Inostroza et al. 2019), and has been proven to be an instrumental tool for studying the impact of human intervention on ecosystems (Arnaiz-Schmitz et al. 2018; Kaminski et al. 2021). Dividing urban areas according to urban–rural gradients and exploring the driving mechanisms of urban wetland evolution under these gradients can help formulate more targeted wetland restoration, protection, and management plans. It also contributes to improving the synergy between urban–rural development and ecological conservation.

In the current research on wetland dynamic changes and driving mechanisms, various statistical approaches are frequently utilized for quantitative evaluation, including but not limited to correlation analysis (Lin et al. 2018; Yi and Wang 2021), cluster analysis (Hu et al. 2021), regression analysis (Wang et al. 2022), principal component analysis (PCA) (Zhang et al. 2021a, b), boosted regression tree (BRT) (Li et al. 2020c), and GeoDetector (Li et al. 2022; Zhang et al. 2021c). In particular, GeoDetector is a collection of statistically based methods constructed to detect spatially stratified heterogeneity and identify its drivers (Wang et al. 2010). It is widely employed to detect ecosystems and their driving mechanisms (Wu et al. 2022). In contrast to other methods, GeoDetector can overcome the limitations of conventional statistical analysis methods and does not need linear assumptions. GeoDetector has proven to be an effective tool for discerning the roles of individual factors and their interactions (Wang and Xu 2017). This approach aligns well with the paper's requirements for the quantitative evaluation of the contributions of individual indicators, encompassing both ecological surroundings and anthropogenic interventions, as well as their interactions. However, since GeoDetector is designed to aptly analyze categorical data, continuous data in driving factors need to be discretized (Wang and Xu 2017). Prior studies typically consult the pertinent literature and existing knowledge to determine the appropriate discretization method and the number of breaks, which influence the precise determination of the outcomes (Wang et al. 2023). In contrast, an optimal parameters-based geographical detector (OPGD) model optimizes the spatial data discretization process and the spatial scales of spatial analysis. It can identify the optimal combination of parameters for the GeoDetector model within a specified range and enhance the precision and efficiency of spatial analysis (Song et al. 2020). Hence, to examine the driving mechanism of wetland dynamic changes, OPGD was utilized in this study.

With its rich wetland resources and excellent protection work, Hefei received the certification of "International Wetland City" (Li et al. 2023) at the 14th Conference of the Parties to the Convention on Ramsar. The certification represents the highest global recognition for the ecological conservation of urban wetlands. Over the past few decades, Hefei has seen substantial and rapid development, increasing the risk of the degradation of wetland areas (Li et al. 2020a). However, existing studies on Hefei's wetlands are primarily centered around the Chaohu Lake area (Li and Gao 2016; Ni et al. 2018; Qiu-yu et al. 2022), lacking a comprehensive assessment of wetland dynamic changes and their driving mechanisms across the Hefei region. As a major city in central China, Hefei is poised to play a crucial role in promoting international wetland protection in the future. A scientific and comprehensive understanding of the dynamic change of Hefei's wetlands and their driving mechanisms is crucial for promoting the protection and development of Hefei's wetlands. Therefore, Hefei was chosen as the study area to investigate the dynamic change characteristics of its wetlands. Additionally, this study investigated the impacts of ecological surroundings and anthropogenic interventions, along with their interactions, on wetland dynamics across different urban–rural gradient regions. This study's primary focus was on (1) analyzing the dynamic characteristics of Hefei's wetlands; (2) constructing landscape indicators that divide urban and rural gradients to quantify the characteristics of Hefei's urban and rural gradients at the landscape scale; and (3) investigating the effects of ecological surrounding and anthropogenic intervention factors, as well as their interactions, on wetland dynamics in regions with different urban–rural gradients in Hefei.

Materials and Methods

Study Area

Hefei (116°41′0″–117°53′0″E, 31°30′0″–32°28′0″N) is situated at the core of Anhui Province (Fig. 1) and spans an area of 11,445 km^2. Hefei consists of four urban

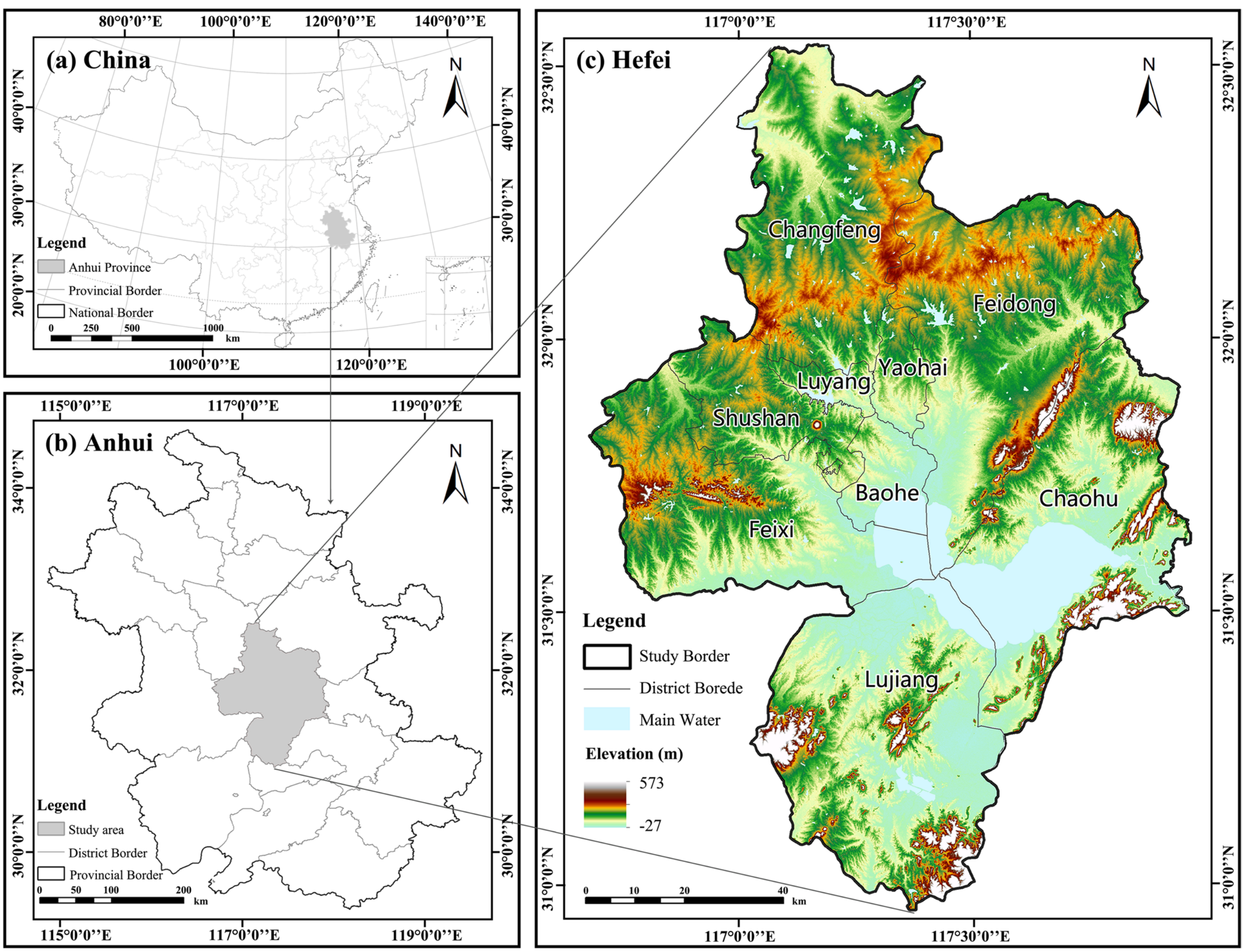

Fig. 1 Location of Hefei

districts, one county-level city, and four counties. Hefei is home to Chaohu Lake, which ranks among China's top five largest freshwater lakes. There are numerous reservoirs, rivers, ponds, and artificial ditches scattered throughout Hefei, making it rich in wetland resources. Hefei currently has 118,200 hectares of wetlands, with a wetland rate of 10.33%. The city experiences a subtropical humid monsoon climate, marked by an average annual temperature of 15.7 °C and an average annual precipitation of around 1,000 mm. In Hefei, climatic conditions manifest substantial heat and precipitation during the summer, contrasting with a temperate winter characterized by significant rainfall. In 2020, the resident population of Hefei grew to 9,369,900 people, its urbanization rate reached 82.3%, and its GDP amounted to 1,004.572 billion yuan. Rapid urbanization poses a severe threat to wetlands. Hence, achieving harmony between economic development and wetland conservation requires a thorough examination of wetland dynamics and the underlying driving forces in Hefei. This is crucial for laying the groundwork for urban planning and safeguarding wetlands.

Data Sources

The data encompass land use data, socioeconomic data, terrain data, soil data, and meteorological data (Table 1). The land use data utilizes the annual China Land Cover Dataset (CLCD). Compared with existing thematic products, CLCD demonstrated commendable consistency (Yang and Huang 2021). The categories of land use were cropland, forest, shrub, grassland, water, snow or ice, wetland, impervious surface, and barren. Considering that paddy fields have lost numerous many of their ecological functions as artificial wetlands, this study does not categorize them as wetlands. This study amalgamates wetlands and water into a unified category termed wetlands.

Socioeconomic data consisted of the annual average population density, Gross Domestic Product (GDP), cropland, and impervious surface proportions. Based on land use data, the proportions of cropland and impervious surface were calculated in ArcGIS Pro (version 3.0.1). Terrain data comprises Digital Elevation Model (DEM), slope, and aspect. Slope and aspect were computed using the Spatial Analysis Tools in ArcGIS Pro (version 3.0.1) based on the DEM data. The soil data utilized consisted of clay, sand, silt, organic

Table 1 Data sources used in this study

Category	Data name	Data format	Time series	Data sources
Land use data	CLCD	Raster, 30 m	1990, 2000, 2010, 2020	https://doi.org/10.5281/zenodo.4417809 (accessed on 11 May 2023)
Socioeconomic data	Annual average population density	Raster, 1 km	1990, 2000, 2010, 2020	Resources and Environmental Science Data Center of the Chinese Academy of Sciences (https://www.resdc.cn/Default.aspx (accessed on 27 June 2023)) and LandScan Global Population Data (https://landscan.ornl.gov/ (accessed on 27 June 2023))
	GDP	Text data	1990, 2000, 2010, 2020	Hefei Statistical Yearbook (https://tjj.hefei.gov.cn/ (accessed on 27 June 2023))
	Cropland proportions Impervious surface proportions	Raster, 30 m	1990, 2000, 2010, 2020	Calculations based on land use data
Terrain data	DEM	Raster, 12.5 m	2009	Earthdata (https://search.earthdata.nasa.gov/ (accessed on 27 June 2023))
	Slope aspect	Raster, 12.5 m	2009	Calculations based on elevation data
Soil data	Clay Sand Silt OC pH	Raster, 1 km	1995	Harmonized World Soil Database (https://www.fao.org/soils-portal/ (accessed on 27 June 2023))
Meteorological data	Monthly average temperature Monthly average precipitation Potential evaporation	Raster, 1 km	1990–2020	National Earth System Science Data Center, National Science & Technology Infrastructure of China (https://www.geodata.cn (accessed on 27 June 2023))

All data were unified to the same geographic coordinates and projection coordinates (geographic coordinates: WGS 1984, projection coordinates: WGS 1984 UTM Zone 50N) carbon (OC), and soil pH. Meteorological data included monthly average temperature, precipitation, and potential evaporation datasets. The average temperatures for each decade during the study period were calculated using the raster calculator in ArcGIS Pro (version 3.0.1).

In this study, to ensure consistency across data with different resolutions during analysis, we preprocessed the datasets. Using ArcGIS Pro (version 3.0.1), we used the Resample tool with the NEAREST method to resample all driving factor data to a uniform 30-m resolution, matching the accuracy of the land use data. All datasets were unified into the same geographic coordinates and projection system (geographic coordinates: WGS 1984, projection coordinates: WGS 1984 UTM Zone 50N).

This study is organized into three major sections, as shown in Fig. 2. Step 1: Analysis of dynamic changes in wetlands. Step 2: Identification of the urban–rural gradient. Step 3: Analysis of the driving mechanism.

Dynamic Change Characteristics of Wetlands

Land Use Transition Matrix

The land use transition matrix involves applying the Markov model to analyze changes in land use, a method commonly utilized to describe modifications in the land use patterns of a specific area. This model can quantitatively characterize the dynamics of land use types across different periods (Shi et al. 2019). The following is its calculation formula:

$$S_{ij} = \begin{bmatrix} S_{11} & S_{12} & \cdots & S_{1n} \\ S_{21} & S_{22} & \cdots & S_{2n} \\ \cdots & \cdots & \cdots & \cdots \\ S_{n1} & S_{n2} & \cdots & S_{nn} \end{bmatrix} \quad (1)$$

where n stands for the overall count of land use categories, where $i, j = 1,2, ..., n$. S_{ij} represents the area converted from type i to type j during the study period.

Single Land Use Dynamic Degree

We chose the model to investigate quantitative alterations in wetlands (Hu et al. 2021). This model examines numerical shifts in a particular kind of land use at a given location over a specified period. The following is the calculating formula:

$$\mathrm{K} = \frac{\mathrm{U_b} - \mathrm{U_a}}{\mathrm{U_a}} \times \frac{1}{\mathrm{T}} \times 100\% \quad (2)$$

where K stand for the dynamic degree; T is the study period in units of years; and U_a and U_b represent the acreages of a particular land use type at the start and end of the research period, respectively.

Urban–Rural Gradient

This study used a clustering indicator based on land cover composition and configuration to define the urban–rural gradient (Kaminski et al. 2021). This method integrates

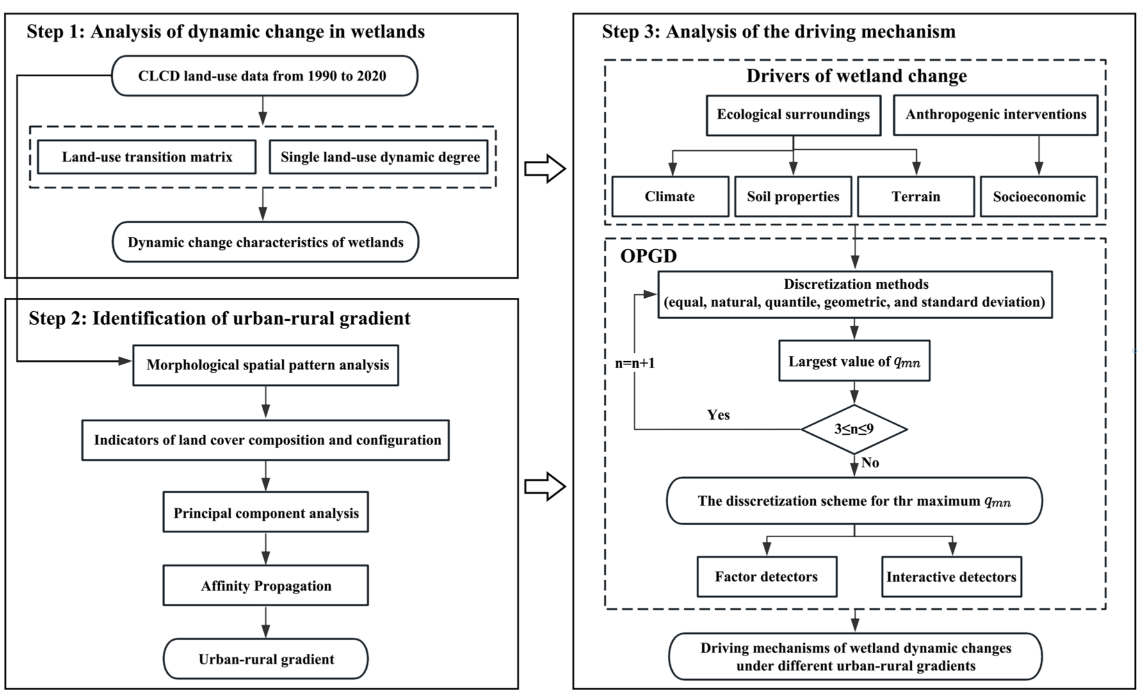

Fig. 2 Overall research framework

landscape pattern indicators, performs clustering to identify gradients, and uses the resulting gradient types to describe administrative units in the study area. More landscape complexity can be captured using this method.

Morphological Spatial Pattern Analysis (MSPA)

MSPA can recognize the spatial topological relationships between target pixel sets and structural elements (Lin et al. 2021). Additionally, there are seven different categories for the identified target pixel sets: core, islet, loop, bridge, perforation, edge, and branch. The literature provides information on the specific meanings and ecological significance of each category (Vogt et al. 2007). MSPA is implemented using the open-source software Guidos Toolbox (version 3.1), which is publicly available at (https://forest.jrc.ec.europa.eu).

This study utilized land use data for this analysis. First, the analysis focused on ecological benefit regions (wetlands and green lands) as foreground, considering other remaining regions as background. Next, the analysis was conducted with developed regions (impervious surfaces) as foreground, with other remaining regions considered as background. Drawing on previous experiences and achievements and taking into account the study area's size parameters, as well as the seven categories regions' numerical patterns (Kaminski et al. 2021), the core type and island type of ecological and built-up areas with a size parameter of 30 m in the MSPA analysis were chosen to represent the key spatial patterns of the city in this study. The towns and streets are selected as the smallest analysis units. Three land use types and four landscape pattern indicators are chosen, and their respective proportions in the analysis unit are calculated to construct a landscape indicator system for urban–rural gradient division, as illustrated in Table 2.

Principal Component Analysis (PCA)

PCA is a commonly used statistical method for dimensionality reduction. It has the capability to distill numerous indicators into a handful of principal components that reflect the majority of information present in the original data (Bro and Smilde 2014). In this study, considering multiple dimensions, a landscape indicator system for urban–rural gradient division is constructed based on land cover composition and configuration. For example, some indicators exhibit a link between ecological land and the ecological land's core region, which makes statistical analysis difficult (Samuelson and Leadbeater 2018). To address this, PCA is applied to the indicator system to reduce dimensionality and extract the main components that characterize urban–rural gradient features. The transformation formula for extracting principal components is as follows:

$$\begin{cases} y_1 = \mu_{11} x_1 + \mu_{12} x_2 + \dots \mu_{1n} x_n \\ y_2 = \mu_{21} x_1 + \mu_{22} x_2 + \dots \mu_{2n} x_n \\ \dots \\ y_k = \mu_{k1} x_1 + \mu_{k2} x_2 + \dots \mu_{kn} x_n \end{cases} \tag{3}$$

where sample x is an n-dimensional random vector $x = (x_1, x_2 \dots x_n)'$ composed of n indicators. There exists a set of vectors μ such that vector x can be transformed into a new k-dimensional composite vector $(y_1, y_2 \dots y_k)'$ through a linear transformation. The newly obtained variable combinations $(y_1, y_2 \dots y_k)'$ become the 1st principal component, 2nd principal component, and so forth until the k-th principal component. The proportion of total variance in y_1 is maximized, and the variance of $y_2 \dots y_k$ decreases sequentially.

Affinity Propagation (AP)

AP is a clustering algorithm in which the basic idea is to consider all data points as potential cluster centers (referred to as exemplars). It constructs a network by connecting each pair of data points with lines, forming a similarity matrix. Then, by propagating messages (responsibility and availability) along the network's edges, it computes the cluster centers for each sample (Frey and Dueck 2007). This algorithm exhibits significantly lower clustering errors than other clustering algorithms and requires less time (Cui et al. 2019). The AP analysis in this study was implemented using the AP from the sklearn package in Python (version 3.9.7). The algorithmic procedure is illustrated in Fig. 3.

Table 2 Landscape indicators and calculation formulas for dividing urban and rural gradients

Landscape indicators	Description
Proportion of impervious surface	$\frac{\text{Impervious surfaces area}}{\text{Urban land area}} \times 100\%$
Proportion of impervious surface's core region	$\frac{\text{Impervious surfaces core region area}}{\text{Urban land area} \times 100\%}$
Proportion of impervious surface's island region	$\frac{\text{Impervious surface's island region area}}{\text{Urban land area} \times 100\%}$
Proportion of ecological land	$\frac{\text{Ecological land area}}{\text{Urban land area}} \times 100\%$
Proportion of ecological land's core region	$\frac{\text{Ecological land's core region area}}{\text{Urban land area}} \times 100\%$
Proportion of ecological land's island region	$\frac{\text{Ecological land's island region area}}{\text{Urban land area}} \times 100\%$
Proportion of cropland	$\frac{\text{Cropland area}}{\text{Urban land area}} \times 100\%$

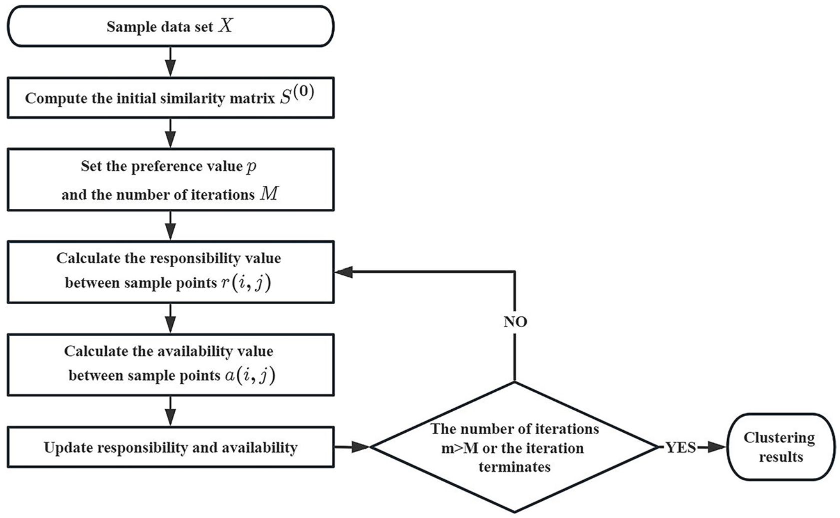

Fig. 3 Affinity Propagation algorithm procedure

Analysis of Driving Mechanisms of Wetland Changes

For this study, 15 factors that contribute to wetland change were chosen based on regional characteristics, data availability, and previous research findings (Li et al. 2022; Wang et al. 2022; Zhang et al. 2023; Zhang et al. 2021a, b; Zhang et al. 2021c). Table 3 provides detailed information on each driving factor. ArcGIS Pro (version 3.0.1) was used to divide the research region into a 250 m × 250 m grid. The wetland degradation area and driving factor data for each grid cell were extracted as the foundational data for the OPGD model. In RStudio (version 4.3.0), the GD package was utilized. By comparing the factor detection q-values for every driving factor, the OPGD model determines the optimal parameter discretization scheme for each driving factor. This study employed five different discretization methods, including equal breaks, natural breaks, quantile breaks, geometric breaks, and standard deviation breaks, with the number of breaks ranging from 3 to 9. The process is illustrated in Fig. 4.

This study utilized the factor and interactive detectors to investigate the driving mechanisms of wetland evolution under different urban–rural gradients. The q-value was used to gauge the explaining power of different drivers on the dependent variable. The formula below is used to calculate q-values:

$$q = 1 - \frac{1}{N\sigma^2}\sum_{h=1}^{L} N_h\sigma_h^2 \tag{4}$$

where $q \in [0,1]$; L represent the number of driver layers; $h = 1, 2, ...L$; N_h and N represent the number of units in layer h and the entire region, respectively; σ_h^2 and σ^2

Table 3 Main parameters of the driving factors used in this study

First-level indicators	Second-level indicators	Third-level indicators	Code	Time series	Resolution
Ecological surroundings	Terrain factors	Elevation	x_1	2009	12.5 m
		Slope	x_2		
		Aspect	x_3		
	Soil factors	Sand	x_4	1995	1 km
		Silt	x_5		
		Clay	x_6		
		OC	x_7		
		pH	x_8		
	Meteorological factors	Average annual precipitation	x_9	1990–2020	1 km
		Average annual potential evapotranspiration	x_{10}		
		Average annual temperature	x_{11}		
Anthropogenic interventions	Socioeconomic factors	GDP	x_{12}	1990/2000/ 2010/2020	1 km
		Population density	x_{13}		
		Proportion of cropland	x_{14}	1990/2000/ 2010/2020	30 m
		Proportion of impervious surface	x_{15}		

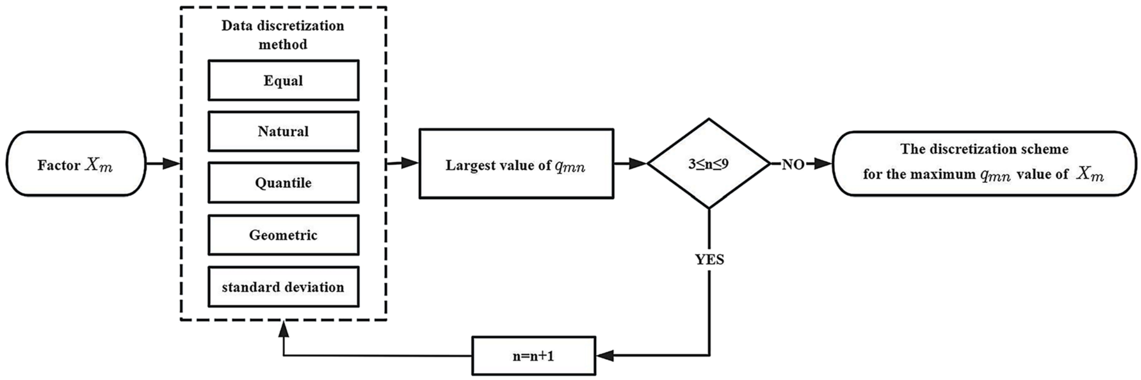

Fig. 4 Optimal data discretization process

represent the variances of the target values in layer h and the entire region. A higher q-value signifies a more pronounced driving effect of the factor, while a lower q-value suggests a weaker effect (Wang et al. 2016).

The interactive detector is employed to detect interactions between drivers. The interactions between two drivers in the interactive detector can be categorized into five types, as shown in Fig. 5.

Results

Wetland Dynamic Changes

In terms of the spatial arrangement of wetlands within Hefei City, Chaohu Lake is the primary feature. Other wetlands are mostly distributed in the southern Huangpi Lake and the northern reservoir area, with some other small wetlands scattered throughout (Fig. 6). In terms of wetland area, there has been a general decline from 1990 to 2020. It first decreased significantly, then increased slightly from 1990 to 2005, followed by a continuous decrease from 2005 to 2020 (Fig. 7). Hefei's wetland area decreased from 1274.56 km^2 in 1990 to 1119.37 km^2 in 2020, with a reduction of 155.19 km^2 in total area and an overall loss of 12.18%. From 1990 to 1995, the wetland area decreased the fastest, from 1274.56 km^2 to 1131.82 km^2, corresponding to a dynamic degree of – 2.24%. From 1995 to 2000, the wetland recovered slightly, increasing from 1131.82 km^2 to 1145.01 km^2, with a wetland dynamic degree of 0.23%. From 2000 to 2005, the wetland recovery growth rate increased from 1145.01 km^2 to 1191.99 km^2, and the wetland dynamic degree was 0.82%. From 2005 to 2020, taking five years as the node, the wetland area displayed a continuing downward trend across the three stages, with slightly different degrees of change, corresponding to dynamic degrees of – 0.38%, – 0.28%, and – 0.59%, respectively (Fig. 8).

In this study, the dynamics of Hefei wetlands were investigated over three time periods (1990–2000, 2000–2010, and 2010–2020). The spatial distribution changes are shown in Fig. 9. The changes in wetlands are mostly due to the decrease caused by the transition of wetlands to farmland and the growth caused by impervious surfaces and the transition of farmland to wetlands. The main bodies of wetland loss are mostly large-area wetlands around Chao Lake and scattered small-area wetlands; the main bodies of wetland increase are mainly Dafangying Reservoir and Huangpi Lake. The wetland restoration and reduction area are shown in Fig. 10, and the source of restoration and the transfer destination of loss are shown in Fig. 11.

Fig. 5 Type of interactions between two driving factors

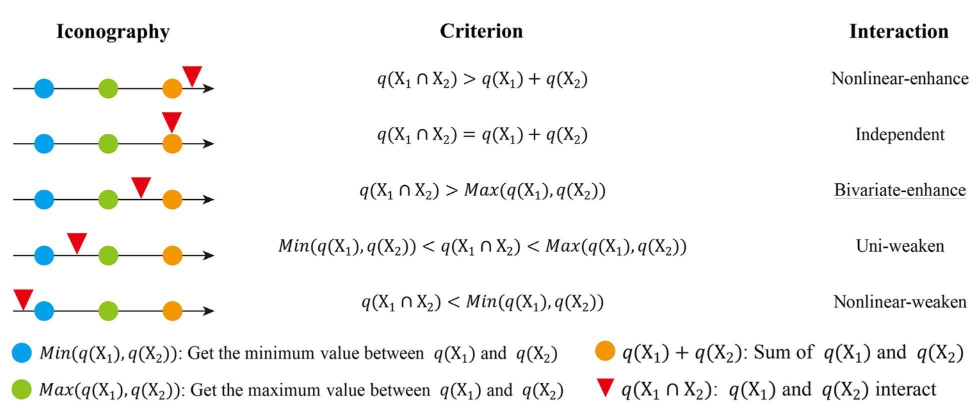

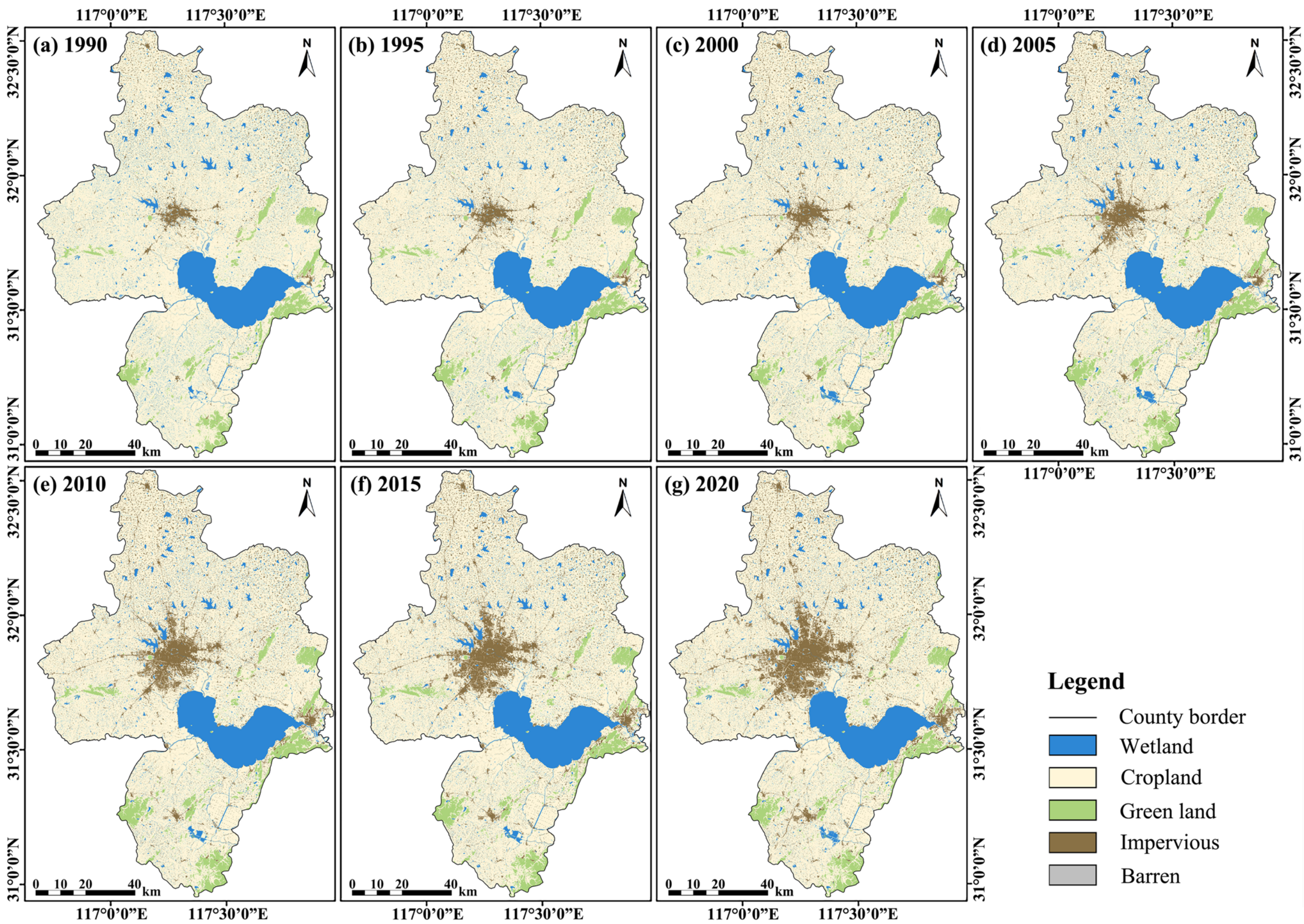

Fig. 6 Spatial distribution changes of wetlands from 1990 to 2020

Fig. 7 Changes in wetland area from 1990 to 2020

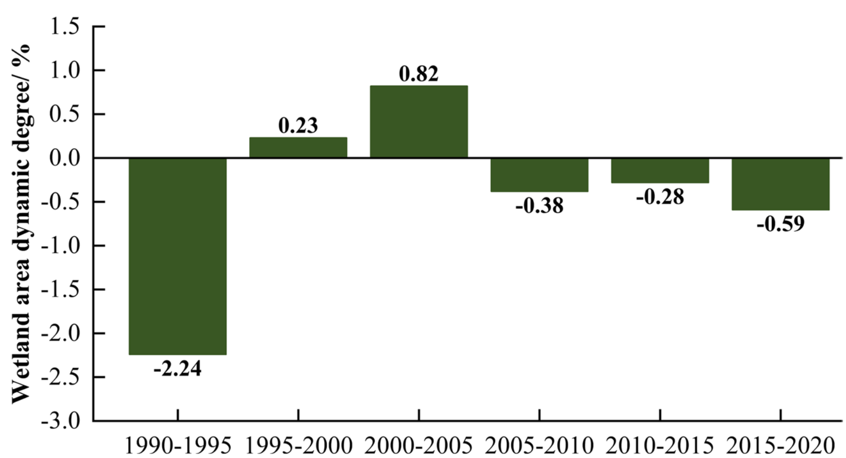

From 1990 to 2000, the wetland area displayed a downward trend, experiencing a loss of 174.00 km^2 and a restoration of 44.46 km^2. The loss area was 129.54 km^2 more than the restoration area. It was mainly converted into farmland and impervious surface, accounting for 164.81 km^2 and 8.92 km^2. From 2000 to 2010, the wetland area exhibited an increasing trend, losing 78.12 km^2 and recovering 102.37 km^2. The restoration area was 24.25 km^2 more than the loss area. This was mainly due to the integration of wetland resources for constructing Dafangying Reservoir and the conversion of farmland and impervious surfaces into wetlands. The respective areas are 94.97 km^2 and 7.34 km^2. From 2010 to 2020, the wetland area displayed a downward trend, experiencing a loss of 109.99 km^2 and a restoration of

Fig. 8 Wetland dynamic degree from 1990 to 2020

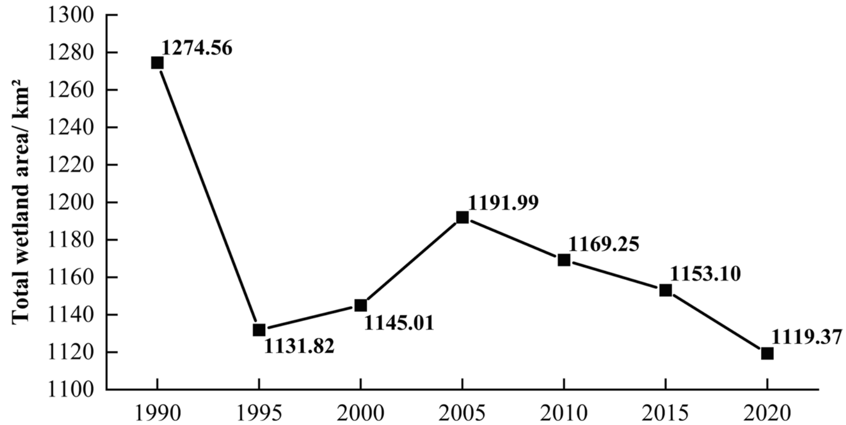

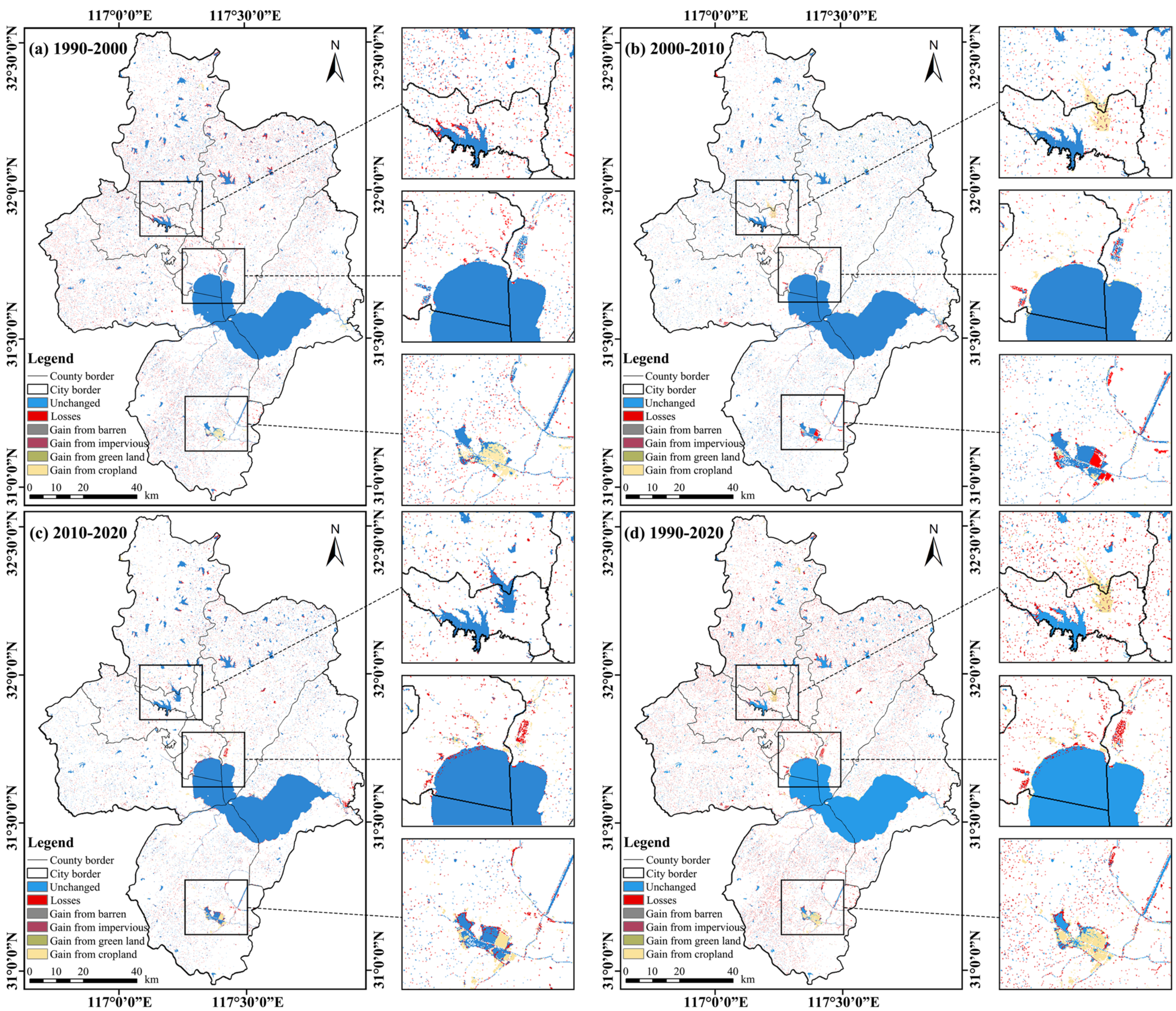

Fig. 9 Spatial distribution map of wetland changes from 1990 to 2020

Fig. 10 Wetland restoration and degradation area from 1990 to 2020

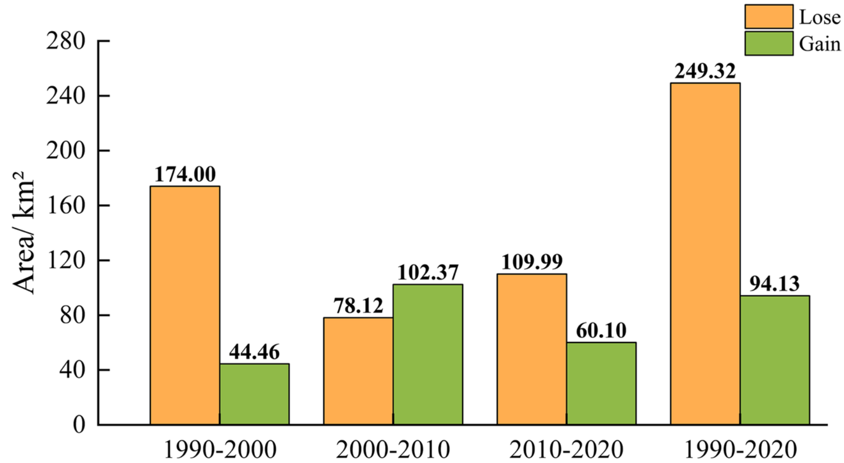

Fig. 11 Sankey diagram of land use transformation from 1990 to 2020

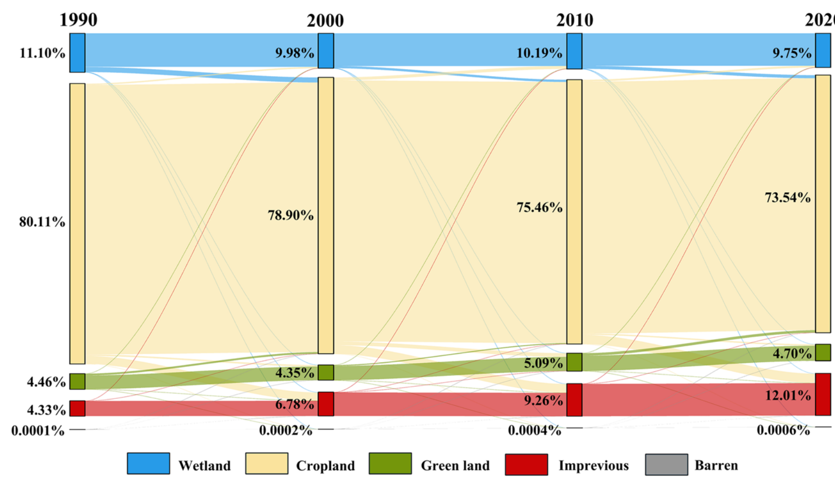

60.10 km^2. The loss area was 49.89 km^2 more than the restoration area, mainly converted into farmland and impervious surface, which were 102.03 km^2 and 7.90 km^2, respectively.

Identifying the Urban–Rural Gradient

Results of the MSPA analysis in Hefei from 1990 to 2020 are shown in Fig. 12. A landscape index system for dividing urban and rural gradients was constructed based on the method described in 2.4.1 above. The PCA results are shown in Table 4. The first three principal components were chosen as inputs to the AP for this study. In 1990, 2000, 2010, and 2020, the first three principal components collectively explained 94%, 97%, 98%, and 98% of the variation in landscape indicators delineating the urban–rural gradient. According to AP clustering data, this study uses the numerical values of urban–rural gradient indicators to identify urban–rural gradient types, divided into four categories: urban areas, agricultural villages, semi-ecological villages, and ecological villages. The spatial distribution of each gradient type is illustrated in Fig. 13. The urban gradient-type regions have the highest proportion of impervious surface, the agricultural village gradient-type regions have the highest proportion of farmland, the semi-ecological village gradient-type regions have the highest proportion of ecological land and cropland, and the ecological village gradient-type regions have the highest proportion of ecological land.

Independent Effects of Each Driving Factor on Wetland Changes

Since the wetland area in Hefei generally exhibited a declining trend from 1990 to 2020, this study used the reduced wetland area as the dependent variable and the 15 driving factors as independent variables. It utilized OPGD to discretize the continuous data within the driving factors. The optimal discretization of the independent variables and the number of breaks are shown in Table A.1. From a single-factor perspective, the explanatory power of each driver is expressed as the q-value. All q-values in the three sub-periods (1990–2000, 2000–2010, 2010–2020) passed the statistical significance test ($p < 0.01$) (Table A.1). The q-values of

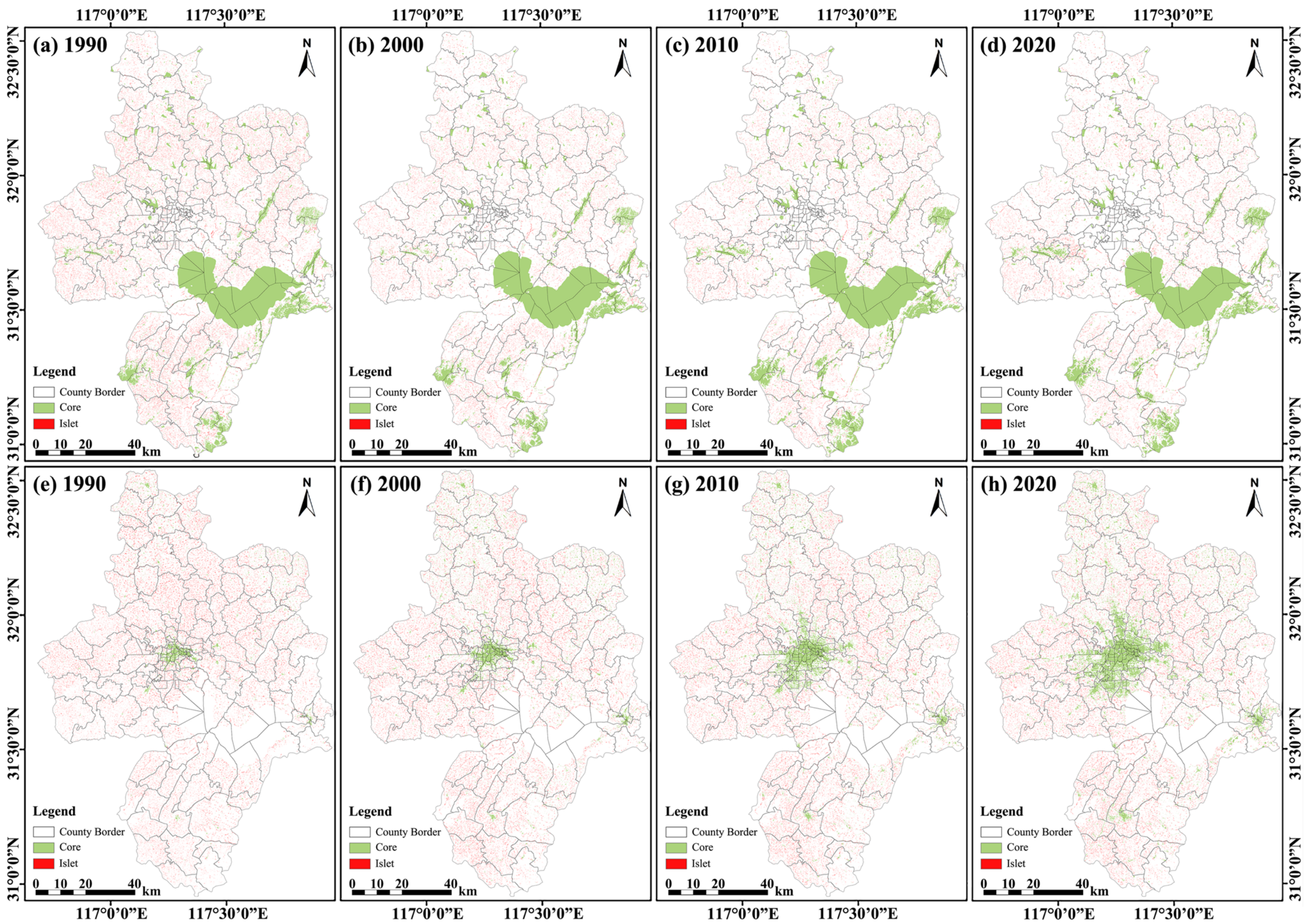

Fig. 12 Results of the MSPA analysis from 1990 to 2020 (a–e are based on using ecological land as the analysis prospect, while e–h are based on using impervious surface as the analysis prospect)

Table 4 Principal component analysis results from 1990 to 2020

		PC1	PC2	PC3	PC4	PC5	PC6
1990	Variance%	46.993	34.713	12.362	5.479	0.32	0.132
	Cumulative variance%	46.993	81.706	94.069	99.548	99.868	100
2000	Variance%	52.393	32.688	11.679	2.878	0.258	0.103
	Cumulative variance%	52.393	85.082	96.761	99.639	99.897	100
2010	Variance%	56.142	30.77	10.79	1.886	0.319	0.093
	Cumulative variance%	56.142	86.912	97.702	99.588	99.907	100
2020	Variance%	58.082	29.363	10.339	1.89	0.233	0.092
	Cumulative variance%	58.082	87.445	97.784	99.674	99.908	100

the driving factors for each period within each urban–rural gradient type region are illustrated in Figs. 14, 15, 16 and 17.

For wetland changes in urban gradient-type regions (Fig. 14), the impervious surface proportion, slope, and aspect exerted significant explanatory power from 1990 to 2000, corresponding to q-values of 0.177, 0.165, and 0.151. While the explanatory capability of pH, OC, clay, and sand exhibited was relatively low, each being below 3%. From 2000 to 2010, OC and sand showed significant explanatory power, corresponding to q-values of 0.390 and 0.347. Furthermore, precipitation, pH, clay, and silt had relatively low explanatory power, all of which were less than 3%. From 2010 to 2020, impervious surface proportion, potential evapotranspiration, and precipitation had notable explanatory power, corresponding to q-values of 0.065, 0.053, and 0.051, respectively. Conversely, pH, OC, clay, silt, sand, and aspect had relatively low explanatory power, all being less than 2%.

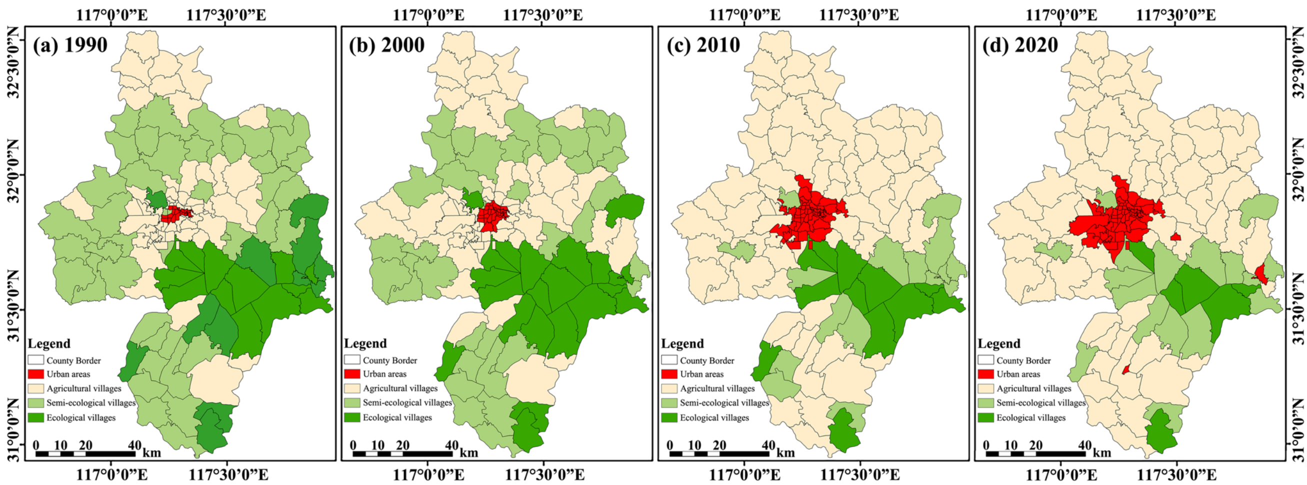

Fig. 13 Spatial distribution of urban–rural gradient types from 1990 to 2020

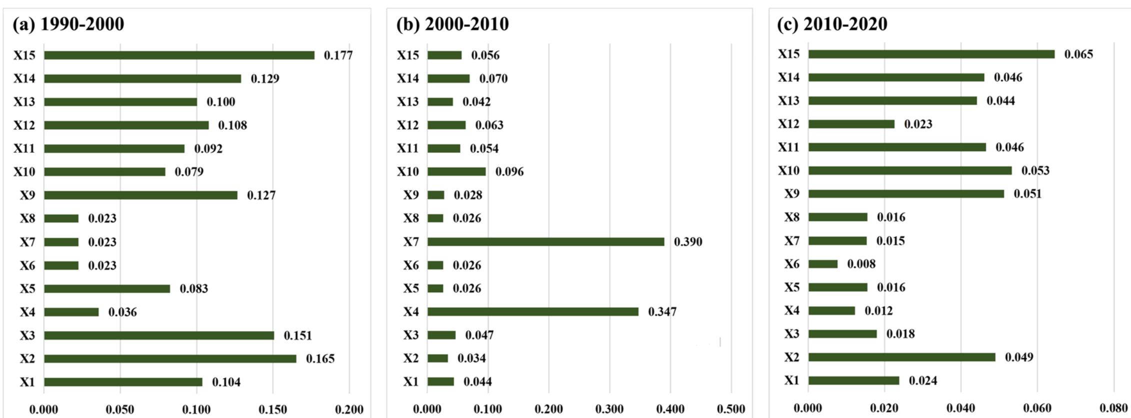

Fig. 14 Explanatory power (q) of driving factors in urban gradient-type regions on wetland changes

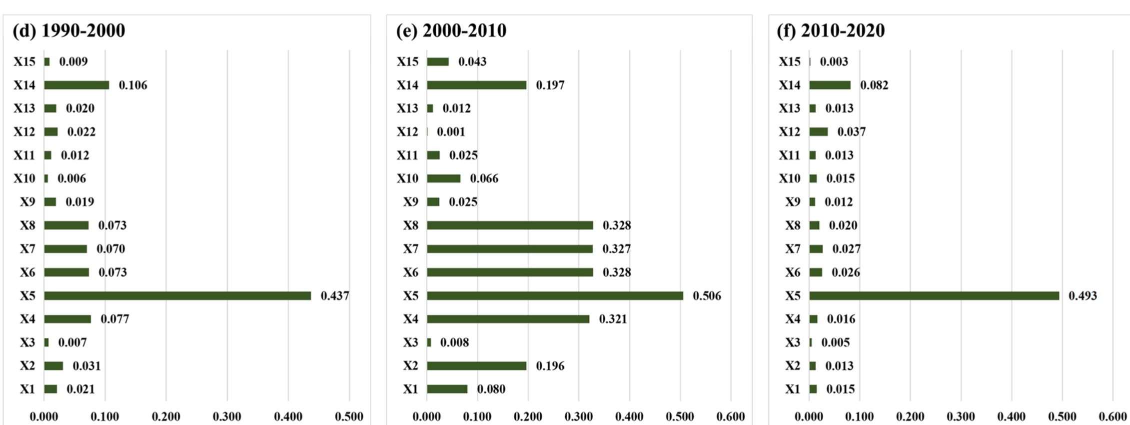

Fig. 15 Explanatory power (q) of driving factors in agricultural village gradient-type regions on wetland changes

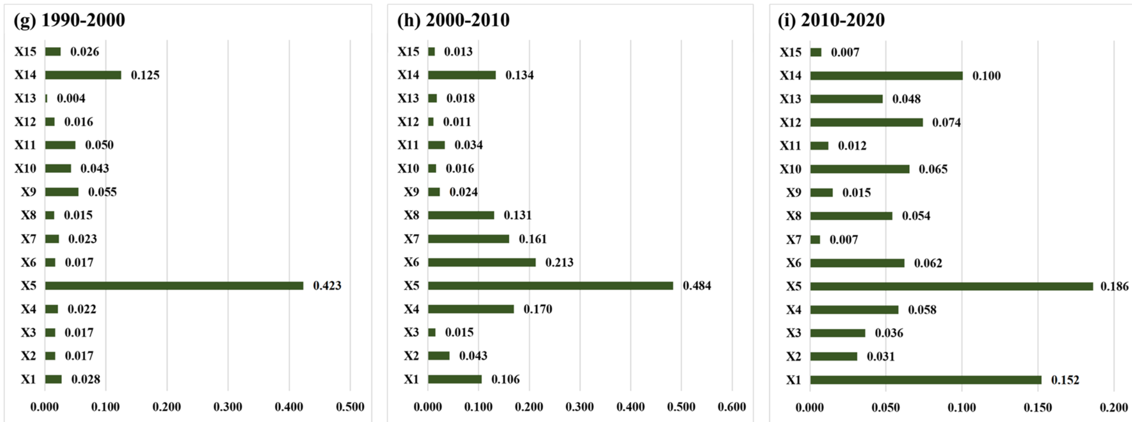

Fig. 16 Explanatory power (q) of driving factors in semi-ecological village gradient-type regions on wetland changes

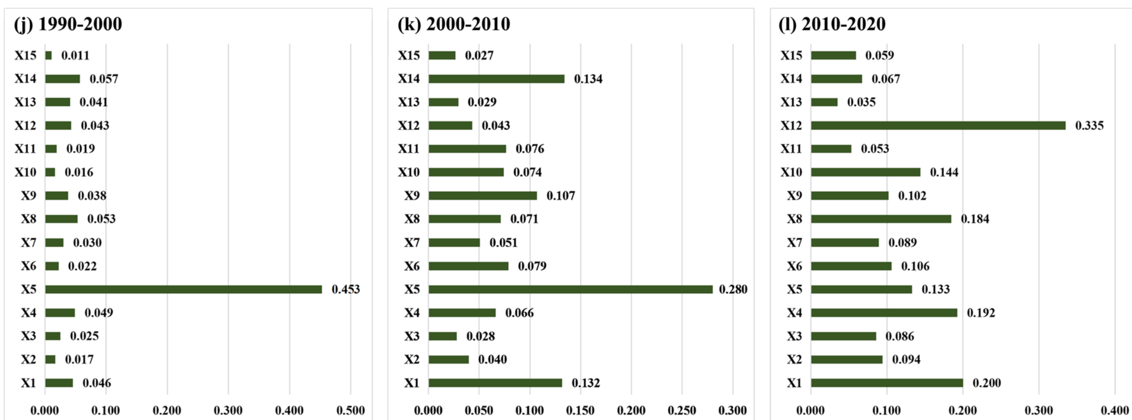

Fig. 17 Explanatory power (q) of driving factors in ecological village gradient-type regions on wetland changes

For wetland changes in agricultural village gradient-type regions (Fig. 15), silt and the cropland proportion exhibited remarkable explanatory power from 1990 to 2000, corresponding to q-values of 0.437 and 0.106. On the contrary, the explanatory powers of the impervious surface proportion, potential evapotranspiration, and aspect were all less than 1%. From 2000 to 2010, silt, pH, clay, OC, and sand demonstrated notable explanatory power, and their corresponding q-values were 0.506, 0.328, 0.328, 0.327, and 0.321. In contrast, population density, GDP, and aspect had relatively low explanatory power, all of which were less than 2%. From 2010 to 2020, silt had the highest explanatory capability. The q-value was 0.493. However, both the impervious surface proportion and aspect had less than 1% explanatory power.

For wetland changes in the semi-ecological village gradient-type regions (Fig. 16), silt and the impervious surface proportions exhibited significant explanatory power from 1990 to 2000, corresponding to q-values of 0.423 and 0.125. In contrast, the explanatory power of population density, GDP, clay, PH, slope, and aspect was relatively low, all below 2%. From 2000 to 2010, the silt and clay demonstrated significant explanatory power, corresponding to q-values of 0.484 and 0.213. However, the impervious surface proportion, population density, GDP, potential evapotranspiration, and aspect had relatively low explanatory power, all of which were less than 2%. From 2010 to 2020, the silt, elevation, and the proportion of cropland demonstrated notable explanatory power, corresponding to q-values of 0.186, 0.152, and 0.100, respectively. In contrast, the explanatory capability of the impervious surface proportion and OC was relatively low, both being less than 1%.

For wetland changes in the ecological village gradient-type regions (Fig. 17), silt exhibited significant explanatory power from 1990 to 2000. The q-value was 0.437. While the impervious surface proportion, temperature, potential evapotranspiration, and slope had explanatory power below 2%. From 2000 to 2010, silt, elevation, precipitation, and cropland proportion demonstrated significant explanatory power, corresponding to q-values of 0.280, 0.132, 0.107, and 0.134. However, the explanatory capability of impervious surface proportion, population density, and aspect were all less than 3%. From 2010 to 2020, GDP and elevation had notable explanatory power, corresponding to q-values of 0.335 and 0.200. Meanwhile, population density exhibited the lowest explanatory power, corresponding to q-value of 0.035.

In summary, among the human-induced factors, the proportion of cropland exhibits strong explanatory power for wetland changes across all four gradient-type regions. Additionally, impervious surface proportion demonstrates notable explanatory power for wetland changes, specifically in urban gradient-type regions. Among the natural factors, soil-related factors play a significant role in explaining wetland changes in rural gradient-type, semi-ecological gradient-type, and ecological village gradient-type regions. Additionally, climate factors show an increasing trend in explanatory power for wetland changes across all four gradient-type regions.

Impact of the Interaction of Driving Factors on Wetland Changes

The reduction of wetland area is not the result of a single factor and requires further explanation by interactive testing. The results of interactive detection indicated that the interactions between the drivers of wetland evolution in Hefei are mainly bivariate-enhance, with a few nonlinear-enhance, uni-weaken, and nonlinear-weaken, and no independent factor effects.

The interactive detection results for urban gradient-type regions are shown in Fig. 18. From 1990 to 2000, 9.52% of interactions exhibited uni-weaken, primarily involving interactions between meteorological factors and soil factors. In addition, 10.47% of interactions were characterized by bivariate-enhance, and the remaining interactions demonstrated nonlinear-enhance. The interaction between the aspect and the proportion of cropland had the strongest effect, corresponding to a q-value of 0.69. Interactions such as elevation ∩ aspect, aspect ∩ GDP, and aspect ∩ impervious surface proportion were also relatively strong, with explanatory power exceeding 60%. From 2000 to 2010, interactions between clay and precipitation exhibited nonlinear-weaken, and 27.62% of interactions showed uni-weaken. This primarily involved the interactions of clay and precipitation with other factors. The remaining interactions demonstrated nonlinear-enhance. The elevation ∩ GDP showing the strongest effect, corresponding to a q-value of 0.32. Interactions such as elevation ∩ precipitation and aspect ∩ proportion of cropland were also relatively strong, with explanatory power exceeding 30%. From 2010 to 2020, interactions between OC and potential evapotranspiration exhibited uni-weaken. Additionally, 8.57% of interactions showed bivariate-enhance, while the remaining interactions demonstrated nonlinear-enhance. The interaction between slope and impervious surface proportions had the strongest effect, corresponding to a q-value of 0.37. Interactions such as slope ∩ potential evapotranspiration, slope ∩ temperature, slope ∩ GDP, slope ∩ proportion of cultivated land, potential evapotranspiration ∩ proportion of cropland, potential evapotranspiration ∩ impervious surface proportion, and temperature ∩ impervious surface proportion were also relatively strong, with explanatory power exceeding 25%. In this gradient-type region, interactions involving soil factors and various factor combinations were generally weak across all three time periods, and some interactions exhibited a weakening trend.

The interactive detection results for agricultural village gradient-type regions are shown in Fig. 19. From 1990 to 2000, 13.33% of interactions exhibited uni-weaken, and 12.38% showed bivariate-enhance, while the remaining interactions demonstrated nonlinear-enhance. The

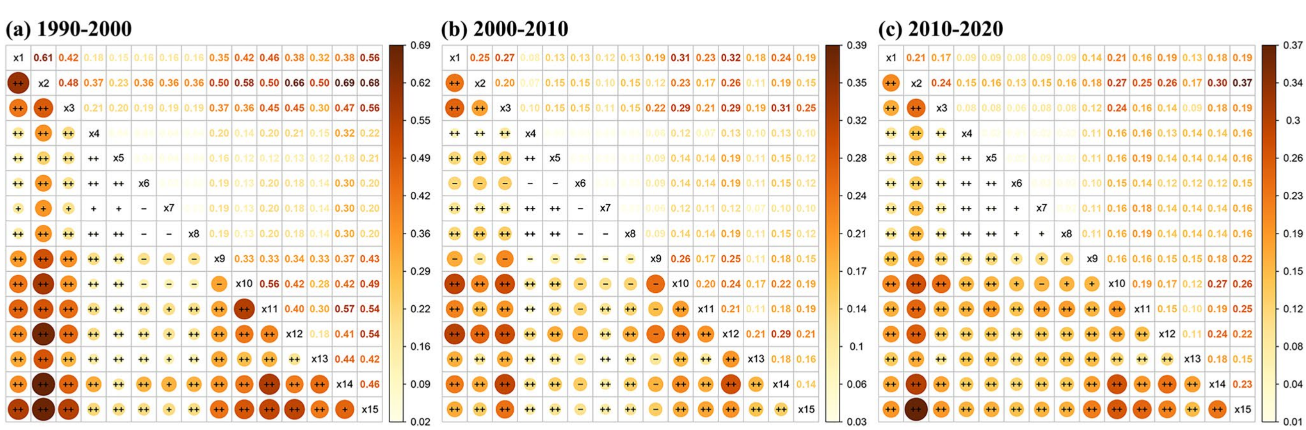

Fig. 18 Interaction results of driving factors in urban gradient-type regions

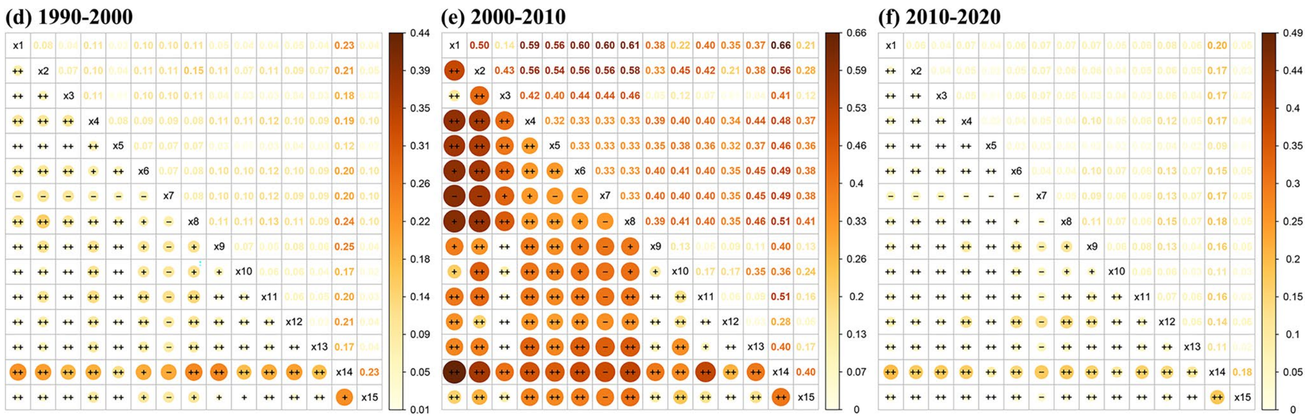

Fig. 19 Interaction results of driving factors in agricultural village gradient-type regions

interaction between precipitation and the proportion of cropland had the strongest effect. The q-value is 0.25. Interactions such as elevation, slope, clay, OC, pH, precipitation, temperature, GDP, and proportion of impervious surface ∩ proportion of cropland were also relatively strong, with explanatory power exceeding 20%. From 2000 to 2010, 11.43% of interactions exhibited uni-weaken, and 12.38% showed bivariate-enhance, while the remaining interactions demonstrated nonlinear-enhance. The interaction between elevation and the proportion of cropland had the strongest effect. The interactions involving the soil factor with other factor combinations were relatively strong, with explanatory power exceeding 30%. From 2010 to 2020, 13.33% of interactions exhibited uni-weaken, and 3.80% showed bivariate-enhance, while the remaining interactions demonstrated nonlinear-enhance. The interaction between elevation and the proportion of cropland had the strongest effect, corresponding to a q-value of 0.20. Interactions such as pH ∩ GDP and slope, aspect, sand, clay, OC, pH, precipitation, temperature, and proportion of impervious surface ∩ proportion of cropland were also relatively strong, with explanatory power exceeding 15%. In this gradient-type region, interactions between the proportion of cropland and various factor combinations were generally strong over the three time periods. However, the interaction between OC and each factor combination was mainly uni-weaken.

The interactive detection results for semi-ecological village gradient-type regions are shown in Fig. 20. From 1990 to 2000, the interaction between OC and pH exhibited nonlinear-weaken, 12.38% of interactions exhibited uni-weaken, and 8.57% showed bivariate-enhance, while the remaining interactions demonstrated nonlinear-enhance. The interaction between the proportion of cropland and impervious surface proportion ∩ precipitation had the strongest effect, with the q-values of both being 0.26. Interactions involving elevation, slope, potential evapotranspiration, temperature, and GDP ∩ proportion of cropland were also relatively strong, with explanatory power exceeding 20%. From 2000 to 2010, 13.33% of interactions exhibited uni-weaken, and 1.90% showed bivariate-enhance, while the remaining interactions demonstrated nonlinear-enhance. The interaction between precipitation and the proportion of cropland had the

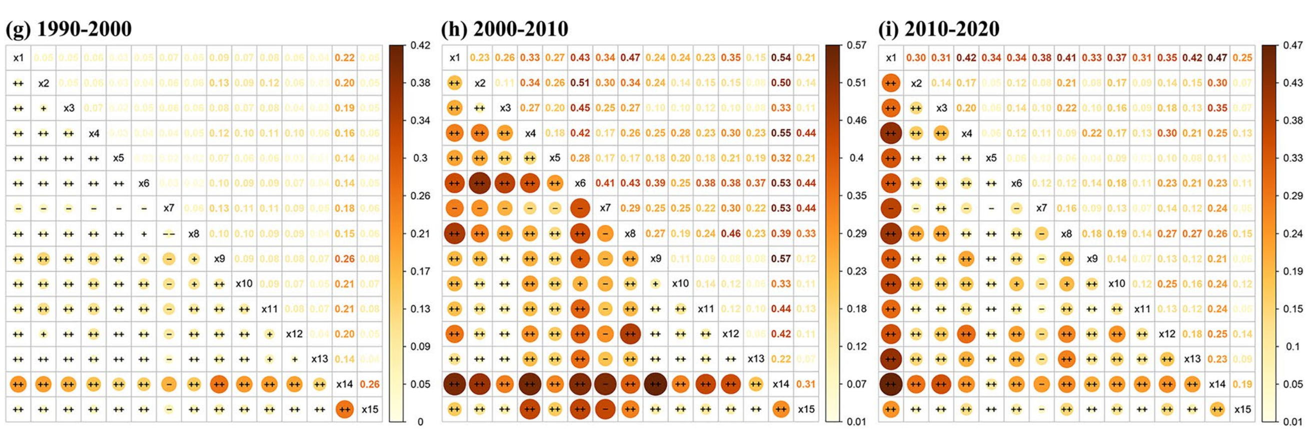

Fig. 20 Interaction results of driving factors in semi-ecological village gradient-type regions

strongest effect, corresponding to a q-value of 0.57. Interactions such as aspect ∩ clay and elevation, slope, sand, clay, OC ∩ proportion of cropland were also relatively strong, with explanatory power exceeding 50%. From 2010 to 2020, 11.43% of interactions exhibited uni-weaken, and 1.90% showed bivariate-enhance, while the remaining interactions demonstrated nonlinear-enhance. The interaction between elevation and the proportion of cropland had the strongest effect, corresponding to a q-value of 0.47. Interactions such as elevation ∩ sand, elevation ∩ pH, and elevation ∩ population density were also relatively strong, with explanatory power exceeding 40%. In this gradient-type region, during 1990–2010, interactions involving the proportion of cropland with various factor combinations were generally strong. From 2010 to 2020, interactions involving both the proportion of cropland and elevation with various factor combinations remained strong. Across all three time periods, interactions involving OC tended to exhibit uni-weaken.

The interactive detection results for ecological village gradient-type regions are shown in Fig. 21. From 1990 to 2000, 13.33% of interactions exhibited uni-weaken, and 5.71% showed bivariate-enhance, while the remaining interactions demonstrated nonlinear-enhance. The interaction between elevation ∩ proportion of cropland had the strongest effect. The associated q-value was 0.19. The interaction between precipitation ∩ proportion of cropland was also relatively strong. The q-value was 0.18. From 2000 to 2010, 13.33% of interactions exhibited uni-weaken, and the remaining interactions demonstrated nonlinear-enhance. The interaction between population density ∩ proportion of cropland had the strongest effect. The associated q-value was 0.59. Interactions involving the proportion of cropland with other factors (excluding silt) were also relatively strong, with explanatory power exceeding 40%. From 2010 to 2020, 13.33% of interactions exhibited bivariate-enhance, while the remaining interactions demonstrated nonlinear-enhance. The interaction between GDP ∩ impervious surface proportion had the strongest effect, corresponding to a q-value of 0.61. The interaction involving GDP with other factors were also relatively strong, with explanatory power exceeding 50%. From 1990 to 2010, the interaction between organic carbon and each factor combination mainly exhibited uni-weaken in this gradient-type region.

Discussion

Dynamic Changing Characteristics of Wetland Landscapes

The interannual variation in wetland area characteristics may be a consequence of Hefei establishing a balance between economic development and resource conservation. During the research period, Hefei's wetland area experienced significant changes (Fig. 7). In the initial stage (1990–1995), as urbanization and industrialization rapidly advanced, Hefei experienced rapid economic development and population growth, which caused extensive wetland loss due to land reclamation and urban infrastructure construction. (Mao et al. 2018). In the following decade (1995–2005), to foster harmonized economic, social, and environmental development, China implemented the “China Wetland Conservation Action Plan” in 2000 and released the “National Wetland Conservation Planning Outline (2002–2003)” in 2003. These initiatives elevated wetland protection and restoration to the national level. Against this background, Hefei has proactively aligned with the national strategy, which has, to a certain extent, reversed the trend of a continuous reduction in wetland area. Meanwhile, the Dafangying Reservoir, built from 2001 to 2004, integrated northern wetland resources, farmland, and impervious surface, which also explains the significant increase in wetland area in Hefei from 2000 to 2005. Although Hefei has made great efforts to protect wetlands in the following 15 years (2005–2020), urban

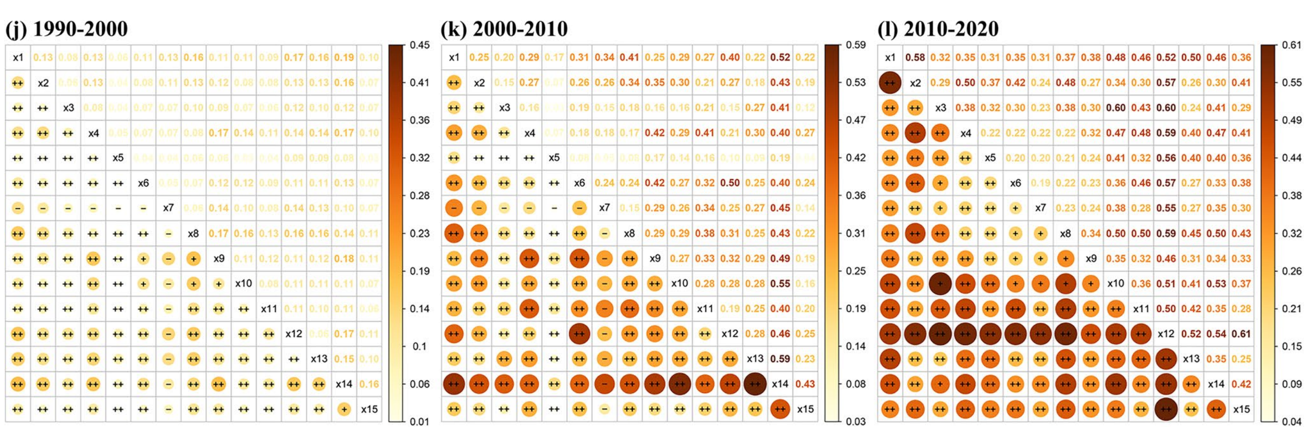

Fig. 21 Interaction results of driving factors in ecological village gradient-type regions

expansion, continued economic and population growth, and other reasons have resulted in a further rise in water demand (Deng et al. 2023), and as a result, the wetland area once again shows a decreasing trend year by year.

Influence of Ecological Surroundings and Anthropogenic Intervention Factors on Urban Wetland Changes Across the Urban–Rural Gradient

The research findings indicate that there are differences in the drivers of wetland change in different urban–rural gradient-type regions. Moreover, the interactions between factors often exhibit greater explanatory power, suggesting that wetland changes are jointly affected by ecological surroundings and anthropogenic interventions (Zhang et al. 2021a, b).

In urban gradient-type regions, anthropogenic interventions have consistently been the dominant factor driving wetland degradation (Fig. 14). The greater the population density, GDP, proportion of impervious surface, and proportion of agricultural land, the more severe the wetland destruction will be (Wang et al. 2022). Regarding ecological surroundings, compared with the situation before 2010, when terrain factors and soil factors were dominant, the influence of climate factors on wetland reduction increased after 2010. Climate changes such as reduced rainfall, increased temperatures, or extreme weather, intensify the reduction of wetlands to some extent (Li et al. 2021, 2020b). In urban gradient-type regions, anthropogenic interference is most severe. Land composition reveals a lesser extent of cultivated and ecological land, with impervious surfaces dominating. The large impervious surface generated by urban construction activities reduces natural land, gradually weakening the explanatory power of soil and topographical factors in influencing wetland changes in this gradient-type region. Therefore, minimizing the negative impact of anthropogenic interventions is key to achieving the sustainable development of wetlands in urban gradient regions.

In contrast, ecological surroundings, particularly soil-related factors, emerge as the predominant drivers of wetland degradation in agricultural village gradient-type regions (Fig. 16). At the same time, the proportion of cropland among anthropogenic intervention has a strong explanatory power regarding the evolution of wetlands in agricultural village gradient-type regions, while the explanatory power of GDP on the evolution of wetlands has increased after 2010. Agriculture village gradient-type regions have more human interference. Land use has more impervious surface, less ecological land, and the most cultivated land. Concentrated agricultural activities directly affect soil properties and quality (Wang et al. 2022); thus, the influence of soil factors on wetland reduction is particularly notable in this gradient-type region. Hefei's economy has developed rapidly since 2010. The encroachment and destruction of wetlands are a result of urban sprawl to meet the demands of urban economic development. Urban expansion has caused the encroachment and disruption of wetlands to accommodate the needs of urban economic development (Mao et al. 2018).

The dominant factors driving wetland degradation are natural in semi-ecological and ecological village gradient-type regions (Figs. 17, 18). Unlike agricultural village gradient-type regions, elevation among natural factors has stronger explanatory power in semi-ecological and ecological village gradient-type regions. The semi-ecological and ecological village gradient-type regions have less human interference and less cultivated land. Among the four urban–rural gradient-type regions, the semi-ecological village gradient-type regions have more ecological land, and the ecological village gradient-type regions have the most ecological land. Most ecological land is natural land, and elevation usually determines the height of the terrain and the direction of water flow. Differences in elevation directly affect the distribution and shape of wetlands (Job and Sieben 2022). Therefore, elevation has a greater explanatory power for wetland changes in these gradient-type regions.

Impact, Limitations, and Prospects

This study explored the differences in how wetland changes respond to ecological surroundings and anthropogenic interventions across different urban–rural gradients based on the OPGD model. This study innovatively introduces urban–rural gradient analysis when analyzing the driving mechanism of wetland evolution. This has significant implications for managing wetlands in urban areas subject to varying levels of anthropogenic interventions and for establishing a balance between economic and social development and wetland conservation.

However, our study still has some limitations to be considered in future research. (1) The dynamic change characteristics of wetlands in Hefei were analyzed in this study based on the CLCD dataset. Limited by the land use classification level of the dataset, this study utilized the first-level classification of land use without further subdivision into the second level for wetlands. This might overlook some information, such as the evolving characteristics and driving mechanisms of different wetland types, potentially affecting the comprehensiveness of the research. (2) This study combines previous research results and data availability, and selects 15 driving factors. However, the drivers may not have been chosen comprehensively enough. For example, anthropogenic interventions are measured from four dimensions: population density, economic growth, changes in the proportion of farmland, and changes in the proportion of impervious surface, without considering the impact of government policies and social culture on the evolution of wetlands. (3) Due to data availability, this study uses soil data from the Second National Land Survey in the World Soil Database. However, soil properties may change during the study period, thus affecting the study's accuracy, but it still provides valuable reference.

In addition, some issues should be discussed in the future. The research results show that the reduction of small-area wetlands in Hefei City is severe (Fig. 9). In the construction process of urban and rural areas, large-area wetlands have received extensive attention due to their outstanding morphological functions and massive impact on people and nature. In contrast, small-area wetlands that are numerous and widely distributed are often overlooked (Liu and Gu 2022). The ecological structure of small-area wetlands is relatively unstable compared to that of large-area wetlands, and rapid urban development poses a significant threat to small-area wetlands (Yuan and Zhou 2022). Small-area wetlands are crucial providers of ecological services; for example, they serve as stepping stones for biological migration and they regulate hydrology and rainfall flooding. They can alleviate the inadequacy of regional ecological resources and the lack of ecological space resulting from the tightness of land resources (Cui et al. 2021; Zhang et al. 2023). Therefore, future studies could further focus on the evolutionary characteristics of small-area wetlands and their driving mechanisms under the urban–rural gradient.

Conclusions

This study analyzed the dynamic changes in wetlands in Hefei and innovatively constructed an urban–rural gradient analysis framework to investigate the driving mechanisms behind wetland dynamics across different urban–rural gradients. First, a single land use dynamic degree and land use transition matrix were used to analyze the dynamic change characteristics of wetlands from 1990 to 2020. Second, combining MSPA, PCA, and AP, we conducted urban–rural gradient identification and delineation. Finally, OPGD was selected to conduct quantitative statistical analysis on the driving forces of factors affecting wetland changes under different urban–rural gradients.

The results indicate that from 1990 to 2020, there have been significant dynamic changes in wetlands in Hefei. The overall trend shows a decrease in wetland area, with a total reduction of 155.19 km^2. This decline primarily manifests in the degradation and disappearance of small wetlands, with wetlands mainly converting to cultivated land and impervious surfaces. The most influential human and natural factors on wetland dynamic changes vary in different urban–rural gradients. In urban gradient-type regions, the primary human and natural factors during 1990–2000 were impervious surface proportion and slope, respectively. In comparison, during 2000–2010, they were the proportion of cropland and potential evapotranspiration. For the period 2010–2020, they were impervious surface proportion and potential evapotranspiration. In agricultural village and semi-ecological village gradient-type regions, the predominant human and natural factors for all three periods were cultivated land ratio and silt. In the ecological village gradient-type regions, the primary human and natural factors for the first two periods were also cultivated land ratio and silt, while for the period 2010–2020, they were GDP and elevation. Additionally, the majority of interactions among driving factors exhibited stronger explanatory power.

This study and its findings provide a basis for understanding and conserving urban wetland resources, balancing urban–rural development and wetland preservation. Additionally, it contributes to advancing the achievement of the United Nations' Sustainable Development Goals by 2030.

Supplementary Information The online version contains supplementary material available at https://doi.org/10.1007/s13157-024-01855-y.

Author Contributions All authors contributed to the study conception and design. Conceptualization: Hui Zhang and Yichen Zhang; methodology: Hui Zhang and Yichen Zhang; software: Hui Zhang; formal analysis: Hui Zhang; investigation: Hui Zhang; resources: Chuntao Li and Lang Zhang; data curation: Hui Zhang; writing—original draft preparation: Hui Zhang; writing—review and editing: Hui Zhang and Yichen Zhang; visualization: Hui Zhang; supervision: Chuntao Li, Yichen Zhang. and Lang Zhang; project administration: Hui Zhang and Chuntao Li; funding acquisition: Lang Zhang All authors have read and agreed to the published version of the manuscript.

Funding This work was supported by the National key R&D project sub-topic (Grant numbers: 2022YFC380260401).

Data Availability The datasets generated during and/or analyzed during the current study are available from the corresponding author on reasonable request.

Declarations

Competing Interests The authors have no relevant financial or non-financial interests to disclose.

References

Arnaiz-Schmitz C, Schmitz MF, Herrero-Jauregui C, Gutiérrez-Angonese J, Pineda FD, Montes C (2018) Identifying socio-ecological networks in rural-urban gradients: Diagnosis of a changing cultural landscape. Sci Total Environ 612:625–635. https://doi.org/10.1016/j.scitotenv.2017.08.215

Bian HL, Li W, Li YZ, Ren B, Niu YD, Zeng ZQ (2020) Driving forces of changes in China's wetland area from the first (1999–2001) to second (2009–2011) National Inventory of Wetland Resources. Global Ecol Conserv 21:8. https://doi.org/10.1016/j.gecco.2019.e00867

Bro R, Smilde AK (2014) Principal component analysis. Anal Meth 6:2812–2831. https://doi.org/10.1039/C3AY41907J

Cong PF, Chen KX, Qu LM, Han JB (2019) Dynamic Changes in the Wetland Landscape Pattern of the Yellow River Delta from 1976 to 2016 Based on Satellite Data. Chin Geogr Sci 29:372–381. https://doi.org/10.1007/s11769-019-1039-x

Cui HF, Wu L, He ZJ, Hu S, Ma K, Yin L, Tao LF (2019) Exploring Multidimensional Spatiotemporal Point Patterns Based on an Improved Affinity Propagation Algorithm. Int J Environ Res Public Health 16:1988. https://doi.org/10.3390/ijerph16111988

Cui LJ, Lei YR, Zhang MY, Li W (2021) Review on small wetlands: definition, typology and ecological services. Acta Ecol Sin 41:2077–2085. https://doi.org/10.5846/stxb202003260699

Davidson NC (2014) How much wetland has the world lost? Long-term and recent trends in global wetland area. Mar Freshw Res 65:934–941

Deng Y, Shao ZF, Dang CY, Huang X, Wu WF, Zhuang QW, Ding Q (2023) Assessing urban wetlands dynamics in Wuhan and Nanchang. China Sci Total Environ 901:15. https://doi.org/10.1016/j.scitotenv.2023.165777

Desta H, Lemma B, Fetene A (2012) Aspects of climate change and its associated impacts on wetland ecosystem functions: A review. J Am Sci 8:582–596. https://doi.org/10.7537/marsjas081012.81

Erwin KL (2009) Wetlands and global climate change: the role of wetland restoration in a changing world. Wetl Ecol Manag 17:71–84. https://doi.org/10.1007/s11273-008-9119-1

Frey BJ, Dueck D (2007) Clustering by passing messages between data points. Science 315:972–976. https://doi.org/10.1126/science.1136800

Havril T, Tóth Á, Molson JW, Galsa A, Mádl-Szőnyi J (2018) Impacts of predicted climate change on groundwater flow systems: can wetlands disappear due to recharge reduction? J Hydrol 563:1169–1180. https://doi.org/10.1016/j.jhydrol.2017.09.020

Herawati A, Syamsiyah J, Baldan S, Arifin I (2021) Application of soil amendments as a strategy for water holding capacity in sandy soils. IOP Conf Ser Earth Environ Sci 724:012014. https://doi.org/10.1088/1755-1315/724/1/012014

Hou L, Wu FQ, Xie XL (2020) The spatial characteristics and relationships between landscape pattern and ecosystem service value along an urban-rural gradient in Xi'an city. China Ecol Indic 108:10. https://doi.org/10.1016/j.ecolind.2019.105720

Hu WM, Li G, Li ZN (2021) Spatial and temporal evolution characteristics of the water conservation function and its driving factors in regional lake wetlands-Two types of homogeneous lakes as examples. Ecol Indic 130:14. https://doi.org/10.1016/j.ecolind.2021.108069

Inostroza L, Hamstead Z, Spyra M, Qureshi S (2019) Beyond urban-rural dichotomies: Measuring urbanisation degrees in central European landscapes using the technomass as an explicit indicator. Ecol Indic 96:466–476. https://doi.org/10.1016/j.ecolind.2018.09.028

Jin XM, Li Y, Fu BL, Yin SB, Yang G, Xing ZF (2017) Spatiotemporal characteristics of wetland to farmland conversion processes in different geomorphological divisions during 1954–2015: a case study in the Sanjiang Plain north of the Wanda Mountains. Acta Ecol Sin 37:3286–3294. https://doi.org/10.5846/stxb201610182121

Job NM, Sieben EJ (2022) Factors controlling wetland formation, Fundamentals of Tropical Freshwater Wetlands. Elsevier 25–41. https://doi.org/10.1016/B978-0-12-822362-8.00021-9

Kaminski A, Bauer DM, Bell KP, Loftin CS, Nelson EJ (2021) Using landscape metrics to characterize towns along an urban-rural gradient. Landsc Ecol 36:2937–2956. https://doi.org/10.1007/s10980-021-01287-7

Kirwan ML, Megonigal JP (2013) Tidal wetland stability in the face of human impacts and sea-level rise. Nature 504:53–60. https://doi.org/10.1038/nature12856

Kumari R, Shukla S, Parmar K, Bordoloi N, Kumar A, Saikia P (2020) Wetlands conservation and restoration for ecosystem services and halt biodiversity loss: An Indian perspective. A Trajectory towards a Sustainable Environment. Springer, Restoration of Wetland Ecosystem, pp 75–85

Li T, Gao X (2016) Ecosystem Services Valuation of Lakeside Wetland Park beside Chaohu Lake in China. Water 8:19. https://doi.org/10.3390/w8070301

Li YY, Liu Y, Ranagalage M, Zhang H, Zhou R (2020a) Examining Land Use/Land Cover Change and the Summertime Surface Urban Heat Island Effect in Fast-Growing Greater Hefei, China: Implications for Sustainable Land Development. ISPRS Int J Geo Inf 9:18. https://doi.org/10.3390/ijgi9100568

Li Z, Jiang WG, Wang WJ, Chen Z, Ling ZY, Lv JX (2020b) Ecological risk assessment of the wetlands in Beijing-Tianjin-Hebei urban agglomeration. Ecol Indic 117:13. https://doi.org/10.1016/j.ecolind.2020.106677

Li Z, Liu M, Hu YM, Xue ZS, Sui JL (2020c) The spatiotemporal changes of marshland and the driving forces in the Sanjiang Plain, Northeast China from 1980 to 2016. Ecol Process 9:13. https://doi.org/10.1186/s13717-020-00226-9

Li HY, Wang JY, Zhang JC, Qin F, Hu JY, Zhou Z (2021) Analysis of Characteristics and Driving Factors of Wetland Landscape Pattern Change in Henan Province from 1980 to 2015. Land 10:15. https://doi.org/10.3390/land10060564

Li ZY, Jiang ZL, Qu YK, Cao YD, Sun FH, Dai YD (2022) Analysis of Landscape Change and Its Driving Mechanism in Chagan Lake National Nature Reserve. Sustainability 14:23. https://doi.org/10.3390/su14095675

Li G, Jiang B, Guan Y, Ramirez-Granada L, Mitsch WJ, Zhang L (2023) Response of soil organic carbon to forested wetlands in East China. Ecol Eng 195:107041. https://doi.org/10.1016/j.ecoleng.2023.107041

Lin WP, Cen JW, Xu D, Du SQ, Gao J (2018) Wetland landscape pattern changes over a period of rapid development (1985–2015) in the ZhouShan Islands of Zhejiang province, China. Estuar Coast Shelf Sci 213:148–159. https://doi.org/10.1016/j.ecss.2018.08.024

Lin JY, Huang CL, Wen YY, Liu X (2021) An assessment framework for improving protected areas based on morphological spatial pattern analysis and graph-based indicators. Ecol Indic 130:9. https://doi.org/10.1016/j.ecolind.2021.108138

Liu HB, Gu XR (2022) Charac teristics and Value of Urban Wetlands —Taking the Central Area of Nanchang as the Example. Chinese Landscape Architecture 38:101–105. https://doi.org/10.19775/j.cla.2022.03.0101

Liu F, Song XF, Yang LH, Han DM, Zhang YH, Ma Y, Bu HM (2018a) Predicting the impact of heavy groundwater pumping on groundwater and ecological environment in the Subei Lake basin, Ordos energy base, Northwestern China. Hydrol Res 49:1156–1171. https://doi.org/10.2166/nh.2017.281

Liu SL, Hou XY, Yang M, Cheng FY, Coxixo A, Wu X, Zhang YQ (2018b) Factors driving the relationships between vegetation and soil properties in the Yellow River Delta, China. Catena 165:279–285. https://doi.org/10.1016/j.catena.2018.02.004

Long XR, Lin H, An XX, Chen SD, Qi SY, Zhang M (2022) Evaluation and analysis of ecosystem service value based on land use/cover change in Dongting Lake wetland. Ecol Indic 136:18. https://doi.org/10.1016/j.ecolind.2022.108619

Maneas G, Makopoulou E, Bousbouras D, Berg H, Manzoni S (2019) Anthropogenic Changes in a Mediterranean Coastal Wetland during the Last CenturyThe Case of Gialova Lagoon, Messinia Greece. Water 11:22. https://doi.org/10.3390/w11020350

Mao DH, Wang ZM, Wu JG, Wu BF, Zeng Y, Song KS, Yi KP, Luo L (2018) China's wetlands loss to urban expansion. Land Degrad Dev 29:2644–2657. https://doi.org/10.1002/ldr.2939

Masood TK, Ali NS (2023) Effect of Different Soil Organic Carbon Content in Different Soils on Water Holding Capacity and Soil Health. IOP Conf Ser Earth Environ Sci 1158:022035. https://doi.org/10.1088/1755-1315/1158/2/022035

McLaughlin DL, Cohen MJ (2013) Realizing ecosystem services: wetland hydrologic function along a gradient of ecosystem condition. Ecol Appl 23:1619–1631. https://doi.org/10.1890/12-1489.1

Meng WQ, He MX, Hu BB, Mo XQ, Li HY, Liu BQ, Wang ZL (2017) Status of wetlands in China: A review of extent, degradation, issues and recommendations for improvement. Ocean Coast Manag 146:50–59. https://doi.org/10.1016/j.ocecoaman.2017.06.003

Newton A, Icely J, Cristina S, Perillo GME, Turner RE, Ashan D, Cragg S, Luo YM, Tu C, Li Y, Zhang HB, Ramesh R, Forbes DL, Solidoro C, Béjaoui B, Gao S, Pastres R, Kelsey H, Taillie D, Nhan N, Brito AC, de Lima R, Kuenzer C (2020) Anthropogenic, Direct Pressures on Coastal Wetlands. Front Ecol Evol 8:29. https://doi.org/10.3389/fevo.2020.00144

Ni J, Xu J, Zhang MJEM (2018) Constructed wetland modelling for watershed ecosystem protection under a certain economic load: A case study at the Chaohu Lake watershed, China. Ecol Model 368:180–190. https://doi.org/10.1016/j.ecolmodel.2017.11.019

Peng KF, Jiang WG, Deng Y, Liu YH, Wu ZF, Chen Z (2020) Simulating wetland changes under different scenarios based on integrating the random forest and CLUE-S models: A case study of Wuhan Urban Agglomeration. Ecol Indic 117:13. https://doi.org/10.1016/j.ecolind.2020.106671

Qiu-yu Z, Peng J, Zhi-qiang Z, Yan-lan W (2022) Evolution and Driving Forces Analysis of Wetland Landscape Pattern around Chaohu Lake from 1975 to 2020. J Yangtze River Sci Res Inst 39:45. https://doi.org/10.11988/ckyyb.20210199

Riaz M, Marschner P (2020) Sandy Soil Amended with Clay Soil: Effect of Clay Soil Properties on Soil Respiration, Microbial Biomass, and Water Extractable Organic C. J Soil Sci Plant Nut 20:2465–2470. https://doi.org/10.1007/s42729-020-00312-z

Salimi S, Almuktar S, Scholz M (2021) Impact of climate change on wetland ecosystems: A critical review of experimental wetlands. J Environ Manage 286:15. https://doi.org/10.1016/j.jenvman.2021.112160

Samuelson AE, Leadbeater E (2018) A land classification protocol for pollinator ecology research: An urbanization case study. Ecol Evol 8:5598–5610. https://doi.org/10.1002/ece3.4087

Shi G, Ye P, Ding L, Quinones A, Li Y, Jiang N (2019) Spatio-Temporal Patterns of Land Use and Cover Change from 1990 to 2010: A Case Study of Jiangsu Province, China. Int J Environ Res Public Health 16:907

Song YZ, Wang JF, Ge Y, Xu CD (2020) An optimal parameters-based geographical detector model enhances geographic characteristics of explanatory variables for spatial heterogeneity analysis: cases with different types of spatial data. GISci Remote Sens 57:593–610. https://doi.org/10.1080/15481603.2020.1760434

van Asselen S, Verburg PH, Vermaat JE, Janse JH (2013) Drivers of Wetland Conversion: a Global Meta-Analysis. PLoS ONE 8:e81292. https://doi.org/10.1371/journal.pone.0081292

Vogt P, Riitters KH, Estreguil C, Kozak J, Wade TG (2007) Mapping spatial patterns with morphological image processing. Landsc Ecol 22:171–177. https://doi.org/10.1007/s10980-006-9013-2

Wang JF, Xu CD (2017) Geodetector: Principle and prospective. Acta Geog Sin 72:116–134. https://doi.org/10.11821/dlxb201701010

Wang JF, Li XH, Christakos G, Liao YL, Zhang T, Gu X, Zheng XY (2010) Geographical detectors-based health risk assessment and its application in the neural tube defects study of the Heshun Region, China. Int J Geogr Inf Sci 24:107–127. https://doi.org/10.1080/13658810802443457

Wang JF, Zhang TL, Fu BJ (2016) A measure of spatial stratified heterogeneity. Ecol Indic 67:250–256. https://doi.org/10.1016/j.ecolind.2016.02.052

Wang GD, Jiang M, Wang M, Xue ZS (2020) Element composition of soils to assess the success of wetland restoration. Land Degrad Dev 31:1641–1649. https://doi.org/10.1002/ldr.3561

Wang C, Ma L, Zhang Y, Chen NC, Wang W (2022) Spatiotemporal dynamics of wetlands and their driving factors based on PLS-SEM: A case study in Wuhan. Sci Total Environ 806:14. https://doi.org/10.1016/j.scitotenv.2021.151310

Wang ZL, Dong C, Dai LD, Wang RY, Liang Q, He LH, Wei D (2023) Spatiotemporal evolution and attribution analysis of grassland NPP in the Yellow River source region. China Ecol Inform 76:20. https://doi.org/10.1016/j.ecoinf.2023.102135

Wu WY, Zhang J, Sun ZY, Yu JA, Liu WJ, Yu R, Wang P (2022) Attribution analysis of land degradation in Hainan Island based on geographical detector. Ecol Indic 141:12. https://doi.org/10.1016/j.ecolind.2022.109119

Xiong Y, Mo SH, Wu HP, Qu XY, Liu YY, Zhou L (2023) Influence of human activities and climate change on wetland landscape pattern-A review. Sci Total Environ 879:11. https://doi.org/10.1016/j.scitotenv.2023.163112

Xue ZS, Hou GL, Zhang ZS, Lyu XG, Jiang M, Zou YC, Shen XJ, Wang J, Liu XH (2019) Quantifying the cooling-effects of urban and peri-urban wetlands using remote sensing data: Case study of cities of Northeast China. Landsc Urban Plann 182:92–100. https://doi.org/10.1016/j.landurbplan.2018.10.015

Yang J, Huang X (2021) The 30 m annual land cover dataset and its dynamics in China from 1990 to 2019. Earth Syst Sci Data 13:3907–3925. https://doi.org/10.5194/essd-13-3907-2021

Yi AL, Wang J (2021) Quantitative study on spatio-temporal evolution and mechanisms of wetland landscape patterns in Shanghai. Acta Ecol Sin 41:2622–2631. https://doi.org/10.5846/stxb202002150262

Yuan Y, Zhou LZ (2022) Dynamic changes in small wetland landscapes and their driving factors under the background of urbanization. Acta Ecol Sin 42:7028–7042. https://doi.org/10.5846/stxb202107061800

Zhang XJ, Wang GQ, Xue BL, Zhang MX, Tan ZX (2021a) Dynamic landscapes and the driving forces in the Yellow River Delta wetland region in the past four decades. Sci Total Environ 787:10. https://doi.org/10.1016/j.scitotenv.2021.147644

Zhang Z, Hu BQ, Jiang WG, Qiu HH (2021b) Identification and scenario prediction of degree of wetland damage in Guangxi based on the CA-Markov model. Ecol Indic 127:13. https://doi.org/10.1016/j.ecolind.2021.107764

Zhang J, Chu L, Zhang Z, Zhu B, Liu X, Yang Q (2023) Evolution of Small and Micro Wetlands and Their Driving Factors in the Yangtze River Delta—A Case Study of Wuxi Area. Remote Sens 15:1152. https://doi.org/10.3390/rs15041152

Zhao GS, Dong JW, Cui YP, Liu JY, Zhai J, He T, Zhou YY, Xiao XM (2019) Evapotranspiration-dominated biogeophysical warming effect of urbanization in the Beijing-Tianjin-Hebei region, China. Clim Dyn 52:1231–1245. https://doi.org/10.1007/s00382-018-4189-0

Zhou DM, Gong HL, Wang YY, Khan SB, Zhao KY (2009) Driving Forces for the Marsh Wetland Degradation in the Honghe National Nature Reserve in Sanjiang Plain, Northeast China. Environ Model Assess 14:101–111. https://doi.org/10.1007/s10666-007-9135-1